EUROPEAN ORGANIZATION FOR NUCLEAR RESEARCH (CERN)

CERN-EP/2016-178
2017/01/06

CMS-EXO-12-055

Search for dark matter in proton-proton collisions at 8 TeV with missing transverse momentum and vector boson tagged jets

The CMS Collaboration*

Abstract

A search is presented for an excess of events with large missing transverse momentum in association with at least one highly energetic jet, in a data sample of proton-proton collisions at a centre-of-mass energy of 8 TeV. The data correspond to an integrated luminosity of 19.7 fb^{-1} collected by the CMS experiment at the LHC. The results are interpreted using a set of simplified models for the production of dark matter via a scalar, pseudoscalar, vector, or axial vector mediator. Additional sensitivity is achieved by tagging events consistent with the jets originating from a hadronically decaying vector boson. This search uses jet substructure techniques to identify hadronically decaying vector bosons in both Lorentz-boosted and resolved scenarios. This analysis yields improvements of 80% in terms of excluded signal cross sections with respect to the previous CMS analysis using the same data set. No significant excess with respect to the standard model expectation is observed and limits are placed on the parameter space of the simplified models. Mediator masses between 80 and 400 GeV in the scalar and pseudoscalar models, and up to 1.5 TeV in the vector and axial vector models, are excluded.

Published in the Journal of High Energy Physics as doi:10.1007/JHEP12(2016)083.

*See Appendix B for the list of collaboration members

1 Introduction

Several astrophysical observations, including those of the radial distribution of galactic rotational speeds [1–3] and the angular power spectrum of the cosmic microwave background [4, 5], suggest an abundance of a nonbaryonic form of matter in the universe. The existence of dark matter (DM) provides some of the most compelling evidence for physics beyond the standard model (SM) of particle physics [6, 7]. In many theories that extend the SM, production of DM particles is expected at the LHC. Monojet searches [8–14] provide sensitivity to a wide range of models for DM production at the LHC, while mono-V (where V=W or Z boson) searches [15–18] target models for DM production associated with SM V-bosons. While the mono-V searches target more specific models, they benefit from smaller SM backgrounds. The interpretation of results from these and other DM searches at the LHC has typically used effective field theories that assume heavy mediators and DM production via contact interactions [19–21]. The results of this analysis are interpreted in the context of a spin-0 or spin-1 mediator decaying to a pair of DM particles, using a set of simplified DM models [22–25] that span a broad range of mediator and DM particle masses, for a specific benchmark point in the model parameter space. In the limit of large mediator masses, these simplified models are well reproduced by the EFT approach. The models provide a simplified description of DM production that is applicable across the full kinematic region accessible at the LHC. Furthermore, within the framework of these models, a straightforward comparison can be made of the limits obtained by LHC experiments with those of direct detection (DD) experiments.

This paper presents a search for new phenomena leading to an excess of events with least one energetic jet and an imbalance in transverse momentum in proton-proton collisions at a centre-of-mass energy of 8 TeV. The data, corresponding to an integrated luminosity of 19.7 fb^{-1}, were collected using the CMS detector at the CERN LHC. This was the first CMS search to target the hadronic decay modes of the V-bosons in the mono-V channels. The mono-V search uses techniques designed to exploit information available in the jet's substructure when the V-boson is highly Lorentz-boosted. Additionally, the search uses a multivariate V-tagging technique to identify the individual jets from moderately boosted V-bosons.

The events are categorized according to the most likely origin of the jets in the event. The signal extraction is performed by considering the missing transverse momentum distribution in each event category, and using multiple data control regions to constrain the dominant backgrounds. These updates to the previous CMS monojet analysis [9] yield improvements of roughly 80% in terms of cross section exclusion limits, using the same data set.

This paper is structured as follows: Section 2 provides a description of the CMS detector and object reconstruction; Section 3 outlines the DM models explored as signal hypotheses; Section 4 provides a description of the event selection and categorization used in the search; Section 5 describes the modelling of backgrounds used in the signal extraction; Section 6 presents the results and interpretations in the context of simplified models for DM production.

2 The CMS detector and object reconstruction

The CMS detector, described in Ref. [26], is a multi-purpose apparatus designed to study high-transverse momentum (p_{T}) products of energetic proton-proton and heavy-ion collisions. A superconducting solenoid surrounds its central region, providing a magnetic field of 3.8 T parallel to the beam direction. Charged-particle trajectories are measured by the silicon pixel and strip trackers, which cover a pseudorapidity (η) region of $|\eta| < 2.5$. A lead tungstate crystal electromagnetic calorimeter (ECAL) and a brass and scintillator hadron calorimeter (HCAL),

surround the tracking volume and cover $|\eta| < 3$. The steel and quartz-fiber Cherenkov forward calorimeter extends the coverage to $|\eta| < 5$. The CMS muon system consists of gas-ionization detectors embedded in the steel flux-return yoke outside the solenoid, covering $|\eta| < 2.4$. The first level of the CMS trigger system, composed of specialized hardware processors, is designed to select the most interesting events in less than 4 μs, using information from the calorimeters and the muon detectors. The high-level trigger processor farm is used to reduce the recorded event rate to a few hundred events per second.

The particle-flow (PF) algorithm reconstructs and identifies each individual particle with an optimized combination of information from the various elements of the CMS detector [27, 28]. Jets are reconstructed by the clustering of PF objects using both the anti-k_{T} algorithm [29] with 0.5 as the distance parameter (AK5), and the Cambridge–Aachen algorithm [30] with 0.8 as the distance parameter (CA8). The jets used in this analysis are required to pass standard CMS identification criteria [31]. The jet momenta are corrected for contamination from additional interactions in the same bunch crossing (pileup) on the basis of the observed event energy density [32]. Further corrections are then applied to calibrate the absolute scale of the jet energy [31].

The missing transverse momentum vector $\vec{p}_{\mathrm{T}}^{\,\mathrm{miss}}$ is defined as the negative vector sum of the p_{T} of all final state particles that are reconstructed using the PF algorithm [33]. The magnitude of $\vec{p}_{\mathrm{T}}^{\,\mathrm{miss}}$ is referred to as $E_{\mathrm{T}}^{\mathrm{miss}}$. Events with a large misreconstructed $E_{\mathrm{T}}^{\mathrm{miss}}$ are removed by applying quality filters on the tracker, ECAL, HCAL, and muon detector data.

3 Signal hypotheses

The signal hypotheses in this search are a set of simplified models for DM production [22–24]. These models assume the existence of an additional particle, a fermionic DM candidate, and an additional interaction that mediates the production of DM. In particular, it is assumed that this additional interaction is mediated by a generic spin-0 or spin-1 particle. The interactions are characterized by four Lagrangians, written for a Dirac-fermion DM particle χ with mass m_{DM}, and a vector (Z′), axial vector (A), scalar (S), or pseudoscalar (P) mediator with mass m_{MED} as,

$$\mathcal{L}_{\text{vector}} \supset \frac{1}{2} m_{\mathrm{MED}}^2 \mathrm{Z}'_\mu \mathrm{Z}'^\mu - g_{\mathrm{DM}} \mathrm{Z}'_\mu \overline{\chi} \gamma^\mu \chi - g_{\mathrm{SM}} \sum_{\mathrm{q}} \mathrm{Z}'_\mu \overline{\mathrm{q}} \gamma^\mu \mathrm{q} - m_{\mathrm{DM}} \overline{\chi} \chi, \tag{1}$$

$$\mathcal{L}_{\text{axial vector}} \supset \frac{1}{2} m_{\mathrm{MED}}^2 \mathrm{A}_\mu \mathrm{A}^\mu - g_{\mathrm{DM}} \mathrm{A}_\mu \overline{\chi} \gamma^\mu \gamma^5 \chi - g_{\mathrm{SM}} \sum_{\mathrm{q}} \mathrm{A}_\mu \overline{\mathrm{q}} \gamma^\mu \gamma^5 \mathrm{q} - m_{\mathrm{DM}} \overline{\chi} \chi, \tag{2}$$

$$\mathcal{L}_{\text{scalar}} \supset -\frac{1}{2} m_{\mathrm{MED}}^2 \mathrm{S}^2 - g_{\mathrm{DM}} \mathrm{S} \overline{\chi} \chi - g_{\mathrm{q}} \sum_{\mathrm{q=b,t}} \frac{m_{\mathrm{q}}}{v} \mathrm{S} \overline{\mathrm{q}} \mathrm{q} - m_{\mathrm{DM}} \overline{\chi} \chi, \tag{3}$$

$$\mathcal{L}_{\text{pseudoscalar}} \supset -\frac{1}{2} m_{\mathrm{MED}}^2 \mathrm{P}^2 - i g_{\mathrm{DM}} \mathrm{P} \overline{\chi} \gamma^5 \chi - i g_{\mathrm{q}} \sum_{\mathrm{q=b,t}} \frac{m_{\mathrm{q}}}{v} \mathrm{P} \overline{\mathrm{q}} \gamma^5 \mathrm{q} - m_{\mathrm{DM}} \overline{\chi} \chi, \tag{4}$$

where $v = 246\,\mathrm{GeV}$ is the SM Higgs potential vacuum expectation value [34]. For the vector and axial vector mediators, the terms g_{DM} and g_{SM} denote the couplings of the mediator to the DM particle and to SM particles, respectively. In all models considered, these couplings are assumed to be unity ($g_{\mathrm{SM}} = g_{\mathrm{DM}} = 1$). For the vector and axial vector mediators, this implies that the coupling is universal between the mediator and quarks of all flavours. For the scalar and pseudoscalar models, $g_{\mathrm{q}} = 1$ is assumed for all quark flavours, which implies a SM Higgs-like coupling of the mediator to the SM fermions. The split in terms of axial vector and vector mediators in the Lagrangian parallels the existing separation in DD experiments,

into spin-dependent (SD) and spin-independent (SI) interactions; SI can refer to either vector or scalar mediated interactions while SD interactions refer to axial vector mediated processes. Pseudoscalar DM-nucleon interaction cross sections are suppressed at non-relativistic DM velocities, leading to a limited sensitivity for DD experiments to this type of interaction [35, 36].

For spin-1 signatures, the DM production process is analogous to Z boson production via quark scattering, as shown in Fig. 2. The mono-V and monojet signatures follow from initial-state radiation (ISR) of a V-boson and quark or gluon, respectively. Constraints on these models for spin-1 mediators can be imposed, based on the results of searches for visible decays of the mediator [37–39], including dijet resonance searches [40]. Typically, dijet resonance searches are interpreted assuming mediator widths that are much smaller than the mediator mass [40–42], while for the coupling parameter values used in this paper, the width of the spin-1 mediator is roughly 40–50% of its mass.

The scalar and pseudoscalar models can be extended by allowing the scalar and pseudoscalar interactions to undergo electroweak symmetry breaking in an analogous way to the Higgs mechanism [43–49]. In such spin-0 models, the coupling of the mediator to SM quarks can be mass-dependent as parameterized in Eqs. (3) and (4). In these models, the production of DM at hadron colliders occurs predominantly through gluon-fusion via a top quark loop as shown in Fig. 1 (left). When couplings of the mediator to vector bosons are present, mono-V signatures are produced through a radiative process, as indicated in Fig. 1 (right). The scenario in which couplings between the mediator and vector bosons are not considered, is denoted herein as *fermionic*. For fermionic models, the mediator width is calculated assuming that it couples only to quarks and DM particles. This is referred to as the minimal width constraint. For the case in which couplings between the mediator and V-bosons are allowed, the width is modified to account for the additional contributions that arise [34].

To model the contributions expected from these signals, simulated events are generated, at leading order (LO) precision, using MCFM 6.8 [50] for the monojet signature and JHUGEN 5.2.5 [51] for the mono-V signature. Large modifications to high-p_{T} production of a spin-0 mediator, produced via gluon-fusion in association with jets, are expected when the actual mass of the top quark is used, rather than assuming it to be infinite [52, 53]. This effect is taken into account in the generation of the scalar and pseudoscalar signals and in the calculation of their cross sections. The NNPDF3.0 set of parton distribution functions (PDF) is used to specify the inputs in the signal generation [54]. The generated events are interfaced with PYTHIA 6.4.26 [55] for parton showering and hadronization with the underlying event tune Z2* [56]. For the monojet signal, the generation is performed using the mediator mass for the renormalization and factorization scales. The mediator mass is also used for the scale in the parton showering (PS).

Higher-order QCD and electroweak effects are not considered in the generation of the monojet signal. Alternative signal samples for the spin-1 mediators, generated with POWHEG 2.0 [57–61] at next-to-leading order (NLO) precision, followed by PYTHIA 8.212 [62] with the underlying event tune CUETP8M1 [63] for the description of fragmentation and hadronization, have been considered. The mediator p_{T} is used, instead of the mediator mass, as the choice for the renormalization, factorization, and PS scales. Using the alternative samples results in a reduction in the expected signal yield of up to 80% for the spin-1 mediators with $m_{\mathrm{MED}} > 400\,\mathrm{GeV}$. Signal samples for the spin-0 mediators were also generated with POWHEG (at LO precision) with the same scale choices as used for spin-1 samples. Using these samples results in a reduced signal yield in the relevant kinematic region, by up to 30% when $m_{\mathrm{MED}} < 400\,\mathrm{GeV}$. The reduction in signal yields predicted by the alternative samples translates to a reduction of the exclusion in the mediator mass by approximately 200 and 20 GeV for small m_{DM} values, for the spin-1

and spin-0 mediators, respectively. Higher-order electroweak effects are expected to reduce the yield of the mono-V signal, for spin-0 mediators, by up to 15% at large mediator p_{T} [64], while NLO QCD corrections are expected to increase the yield by roughly 25% [65].

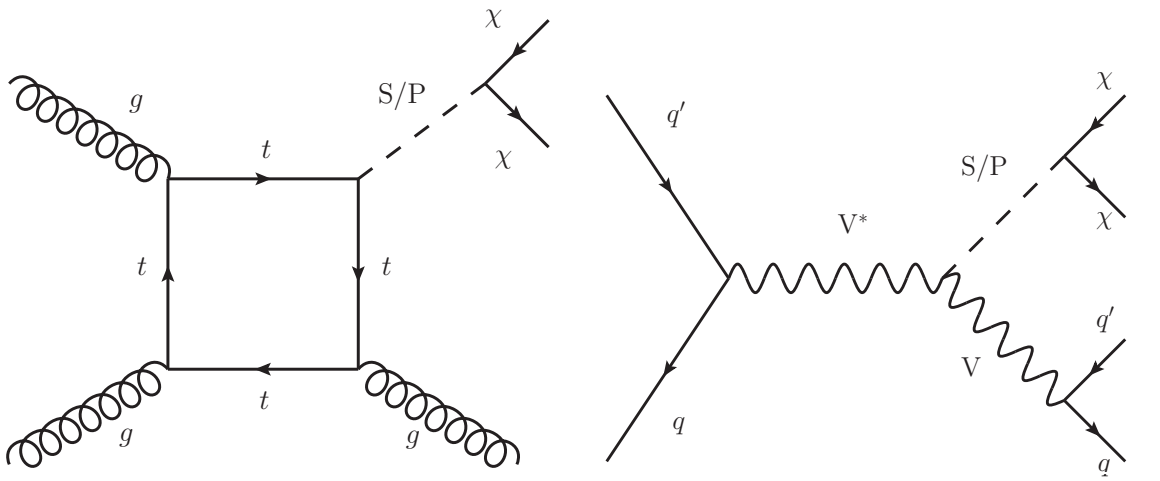

Figure 1: Diagrams for production of DM via a scalar (S) or pseudoscalar (P) mediator in the cases providing monojet (left) and mono-V (right) signatures.

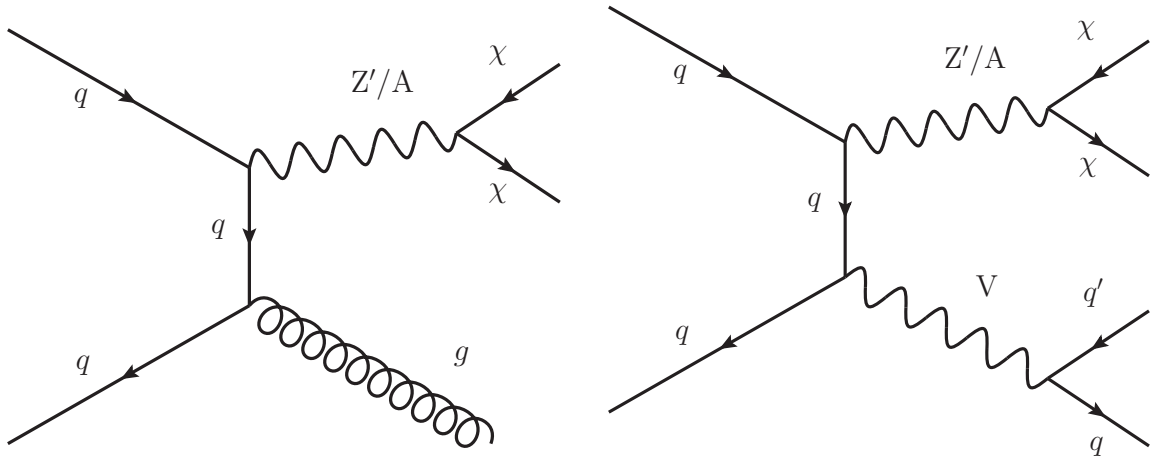

Figure 2: Diagrams for production of DM via a vector (Z′) or axial vector (A) mediator providing monojet (left) and mono-V (right) signatures.

To compute the SM background expectation, simulated samples are produced at LO for the $\mathrm{Z}+$jets, $\mathrm{W}+$jets, $\mathrm{t\bar{t}}$, and QCD multijet processes using MADGRAPH 5.1.3 [66] interfaced with PYTHIA 6.4.26 for hadronization and fragmentation, where jets from the matrix element calculations are matched to the parton shower, following the MLM matching prescription [67]. Additionally, a single top quark background sample is produced at NLO with POWHEG 1.0, and a set of diboson and $\gamma+$jets samples are produced at LO with PYTHIA 6.4.26. All of the simulated background samples are generated using the CT10 PDF set [68]. The underlying event description is provided by the Z2* tune in the signal and background simulation.

The generated signal and background events are interfacted with GEANT4 [69] to simulate the CMS detector response. The simulated samples are then corrected to account for the distribution of pileup interactions observed in the 8 TeV data set. All signal and background samples are additionally corrected to account for the observed mismodelling of hadronic recoil in simulation, following the procedure described in Ref. [33].

4 Event selection and categorization

Candidate signal events are selected by requiring large values of $E_{\mathrm{T}}^{\mathrm{miss}}$ and one or more high-p_{T} jets. The data used for this analysis are collected using two $E_{\mathrm{T}}^{\mathrm{miss}}$ triggers. The first requires $E_{\mathrm{T}}^{\mathrm{miss}} > 120\,\mathrm{GeV}$, where the $E_{\mathrm{T}}^{\mathrm{miss}}$ is calculated using a PF reconstruction algorithm that only uses information from the calorimeters, while the second requires $E_{\mathrm{T}}^{\mathrm{miss}} > 95\,\mathrm{GeV}$ or $E_{\mathrm{T}}^{\mathrm{miss}} > 105\,\mathrm{GeV}$, depending on the data taking period, together with at least one jet with $p_{\mathrm{T}} > 80\,\mathrm{GeV}$ and $|\eta| < 2.6$.

Selected events are required to have $E_{\mathrm{T}}^{\mathrm{miss}} > 200\,\mathrm{GeV}$ to ensure a trigger efficiency greater than 99% for all events used in the analysis. The azimuthal angle ϕ between the $\vec{p}_{\mathrm{T}}^{\mathrm{miss}}$ and the highest-p_{T} (leading) jet, $|\Delta\phi(\vec{p}_{\mathrm{T}}^{\mathrm{miss}}, \mathrm{j})|$, is required to be larger than 2 radians to reduce the contribution from QCD multijet events. Events are vetoed if they contain at least one well-identified electron, photon, or muon with $p_{\mathrm{T}} > 10\,\mathrm{GeV}$, or a τ lepton with $p_{\mathrm{T}} > 15\,\mathrm{GeV}$ [70–73]. The electron, τ lepton, and photon vetoes require that the identified object be isolated, by using standard PF isolation algorithms [74].

Selected events are classified according to the topology of the jets to distinguish between ISR of a quark or gluon, and hadronic V-boson decays, which can be either highly Lorentz-boosted or resolved into two jets. This approach results in three independent classes of events that are referred to as the monojet, V-boosted, and V-resolved categories. The V-boosted and V-resolved categories are collectively referred to as the V-tagged categories.

If the V-boson decays hadronically and has sufficiently large p_{T}, both of its hadronic decay products are captured as a single reconstructed "fat" jet. Events in this V-boosted category are required to have a reconstructed CA8 jet with $p_{\mathrm{T}} > 200\,\mathrm{GeV}$ and $E_{\mathrm{T}}^{\mathrm{miss}} > 250\,\mathrm{GeV}$. Additional selection criteria are applied to improve the vector boson jet purity by cutting on the "N-subjettiness" ratio τ_2/τ_1 as defined in Refs. [75, 76], which identifies jets with a two-subjet topology, and on the pruned jet mass (m_{pruned}) [77]. The τ_2/τ_1 ratio is required to be smaller than 0.5 and m_{pruned} is required to be in the range 60–110 GeV. Events which contain additional AK5 jets close to the CA8 jet, but no closer than $\Delta R = \sqrt{(\delta\eta)^2 + (\delta\phi)^2} = 0.5$, are selected to include the frequent cases in which ISR yields additional jets. If exactly one AK5 jet with $p_{\mathrm{T}} > 30\,\mathrm{GeV}$ and $|\eta| < 2.5$ is reconstructed with $\Delta R > 0.5$ relative to the CA8 jet, and the azimuthal angle between it and the CA8 jet is smaller than 2 radians, the event is selected. Events with more than one AK5 jet with $p_{\mathrm{T}} > 30\,\mathrm{GeV}$ and $|\eta| < 2.5$, reconstructed at $\Delta R > 0.5$ relative to the CA8 jet, are rejected. Figure 3 shows the distributions in τ_2/τ_1 and m_{pruned} before the application of the jet mass selection, in simulation and data, for the V-boosted category. A discrepancy is present in the simulation relative to the data. This discrepancy has been studied and found to fall within the variations observed when using different parton shower models and detector descriptions in the simulation [78]. The disagreement is within the systematic uncertainties of the selection efficiency that are included in this analysis.

In cases where the V-boson has insufficient boost for its hadronic decay to be fully contained in a single reconstructed CA8 jet, a selection that targets V-boson decays into a pair of AK5 jets is applied to recover events failing the V-boosted selection. This selection requires that each jet has $p_{\mathrm{T}} > 30\,\mathrm{GeV}$ and $|\eta| < 2.5$, and that the dijet system has a mass in the range 60–110 GeV, consistent with originating from a W or Z boson. To reduce the combinatorial background in this V-resolved category, a multivariate (MVA) selection criterion is applied. The inputs to the MVA are the jet pull angle [79], the mass drop variable [80], and a likelihood-based discriminator that distinguishes quark-originated from gluon-originated jets [81]. In events where multiple dijet pairs are found, the pair with the highest MVA output value is taken as the candidate.

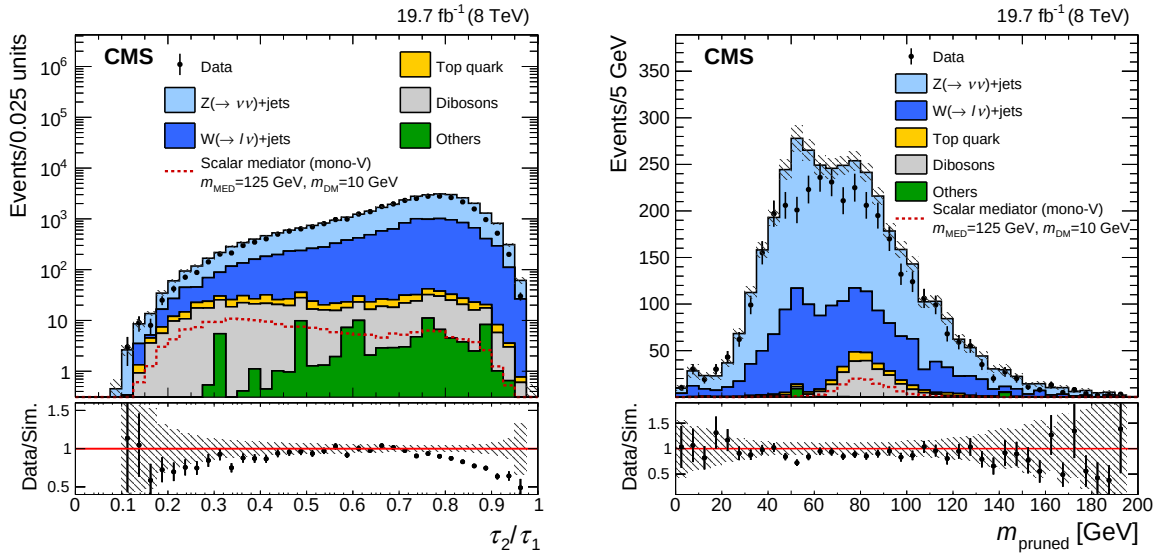

Figure 3: Left: The distribution of τ_2/τ_1 in highly Lorentz-boosted events, before the jet mass selection. Right: The distribution of m_{pruned} for the CA8 jets, before applying the jet mass selection but after the requirement of $\tau_2/\tau_1 < 0.5$ has been applied. The discrepancy between data and simulation is within systematic uncertainties (not shown). The dashed red line shows the expected distribution for scalar-mediated DM production with $m_{\text{MED}} = 125\,\text{GeV}$ and $m_{\text{DM}} = 10\,\text{GeV}$. The shaded bands indicate the statistical uncertainty from the limited number of simulated events.

The distributions of the MVA output for SM backgrounds and for a scalar mediator produced in association with a V-boson are shown in Fig. 4. The disagreement observed between the data and simulation is included as a systematic uncertainty in the efficiency of the V-resolved category selection for the top quark and diboson backgrounds. Events are included in the V-resolved category if they have an MVA output greater than 0.6. This selection is optimal for mono-V signals with a spin-0 mediator with $m_{\text{MED}} < 300\,\text{GeV}$ [81].

To reduce contamination from top quark backgrounds, events are rejected if they contain a jet that is identified as a b jet, defined using the combined secondary vertex tagger operating at a medium efficiency working point [82]. Finally, the events are required to have $E_{\text{T}}^{\text{miss}} > 250\,\text{GeV}$.

Events that do not qualify for either of the two V-tagged categories are required to have one or two high-p_{T} jets that are consistent with originating from a single quark or gluon. This final category is referred to as the monojet category. For the monojet category, events are required to have $E_{\text{T}}^{\text{miss}} > 200\,\text{GeV}$ and contain at least one AK5 jet within $|\eta| < 2$ with $p_{\text{T}} > 150\,\text{GeV}$. Events containing a second AK5 jet with $p_{\text{T}} > 30\,\text{GeV}$ and $|\eta| < 2.5$ are selected, providing the azimuthal angle between the leading jet with $|\eta| < 2$ and this second AK5 jet is less than 2 radians. This selection recovers the frequent cases where ISR yields two jets in the monojet signal. Events with three or more AK5 jets with $p_{\text{T}} > 30\,\text{GeV}$ and $|\eta| < 2.5$ are rejected. Table 1 gives a summary of the event selection in the three categories. The priority for event selection is that events are first selected in the V-boosted category, followed by the V-resolved category, and finally in the monojet category. Events which pass a given selection are not included in any subsequent category.

Figure 5 shows the $E_{\text{T}}^{\text{miss}}$ and leading jet p_{T} distributions in data and simulation after selection for the three event classes combined. The backgrounds are normalized to the integrated luminosity of the data samples, and the expected distribution for vector mediated DM production

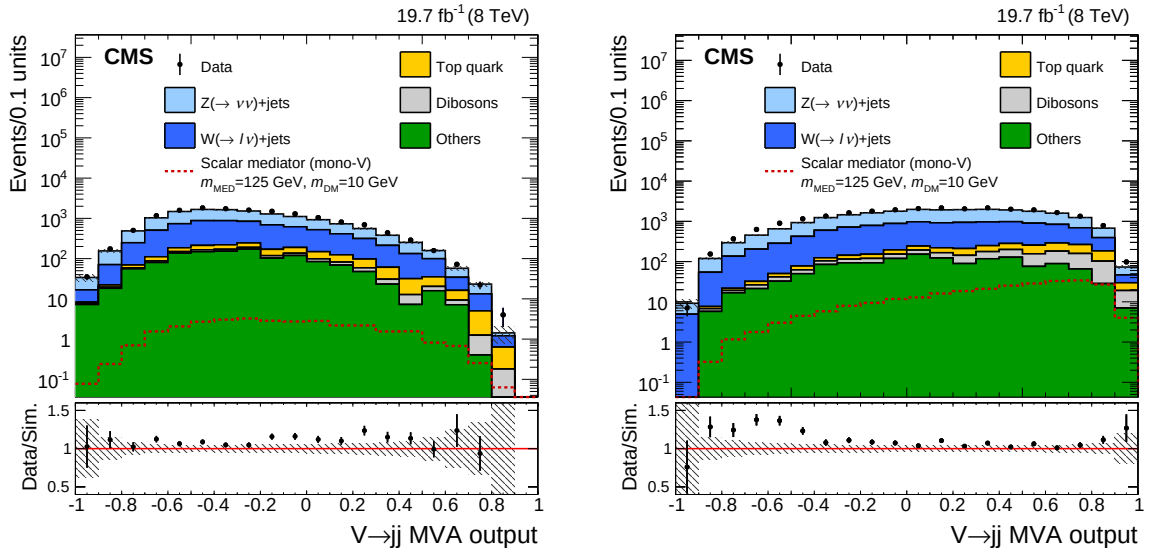

Figure 4: The MVA output distributions for V-tagged events in simulation and data after signal selection for $p_{\mathrm{T}} < 160\,\mathrm{GeV}$ (left) and $p_{\mathrm{T}} > 160\,\mathrm{GeV}$ (right). Above a p_{T} of about 160 GeV, the jets from the V-boson decay begin to overlap. The dashed red line shows the expected distribution for scalar-mediated DM production with $m_{\mathrm{MED}} = 125\,\mathrm{GeV}$ and $m_{\mathrm{DM}} = 10\,\mathrm{GeV}$. The shaded bands indicate the statistical uncertainty arising from the limited number of simulated events.

assuming m_{DM} =10 GeV and m_{MED} =1 TeV is overlaid. The discrepancy between the data and simulation is a result of both detector resolution and an imperfect theoretical description of the kinematics of the V + jets processes. Both effects are corrected using control samples in data, as described in the following section.

5 Background estimation

The presence of DM production would be observable as an excess of events above SM backgrounds at high $E_{\mathrm{T}}^{\mathrm{miss}}$. The sensitivity obtained by considering the shape of the $E_{\mathrm{T}}^{\mathrm{miss}}$ spectrum in these events is significantly better than that achieved in the simple counting analysis described in the previous CMS paper [9]. Additional improvement is achieved by using control regions in data to reduce the uncertainties in the predictions of the SM backgrounds. These regions are statistically independent from the signal region and designed such that the expected contribution from a potential signal is negligible. A binned likelihood fit is performed in the ranges 250–1000 GeV and 200–1000 GeV for the two V-tagged and monojet categories, respectively. The binning is chosen to ensure that each corresponding bin of a set of control regions is populated. The width of the highest $E_{\mathrm{T}}^{\mathrm{miss}}$ bin is chosen to provide ease of comparison with the previous CMS search [9].

The background contributions from $\mathrm{Z}(\nu\nu)$ + jets and $\mathrm{W}(\ell\nu)$ + jets are determined using data from dimuon and photon, and single muon control regions, respectively. The events in the control regions are divided into the three categories, using the selection criteria described in Section 4, but replacing the lepton and photon vetoes with a requirement of the presence of one of the following: a pair of oppositely charged muons consistent with a Z boson decay, a high p_{T} photon, or a single muon consistent with a leptonic W boson decay. This yields a total of nine control regions; three for each event category. In the control regions, the transverse momentum of the dimuon pair, the single muon, or the photon is removed and the $E_{\mathrm{T}}^{\mathrm{miss}}$ is

Table 1: Event selections for the V-boosted, V-resolved, and monojet categories The requirements on $p_{\mathrm{T}}^{\mathrm{j}}$ and $|\eta|^{\mathrm{j}}$ refer to the highest p_{T} CA8 or AK5 jet in the V-boosted or monojet categories, and to both leading AK5 jets in the V-resolved category. The requirement on the number of jets (N_{j}) is applied in the V-boosted and monojet categories. An additional jet is allowed only if it falls within $|\Delta\phi| < 2$ radians of the leading AK5 or CA8 jet for the monojet or V-boosted category. The additional AK5 jets in the V-boosted category must be further than $\Delta R > 0.5$ for the event to fail this criteria.

	V-boosted	V-resolved	Monojet
$p_{\mathrm{T}}^{\mathrm{j}}$	>200 GeV	>30 GeV	>200 GeV
$\lvert\eta\rvert^{\mathrm{j}}$	<2.5	<2	<2
$E_{\mathrm{T}}^{\mathrm{miss}}$	>250 GeV	>250 GeV	>200 GeV
τ_2/τ_1	<0.5	—	—
$\mathrm{V} \to \mathrm{jj}$ MVA output	—	>0.6	—
m_{pruned}	60–110 GeV	—	—
m_{jj}	—	60–110 GeV	—
$\lvert\Delta\phi(\vec{p}_{\mathrm{T}}^{\mathrm{miss}}, \mathrm{j})\rvert$	>2 rad	—	>2 rad
$\mathrm{N_j}$	=1	—	=1

recalculated. This quantity is referred to as pseudo-$E_{\mathrm{T}}^{\mathrm{miss}}$ and it is this variable to which the $E_{\mathrm{T}}^{\mathrm{miss}}$ selection of the corresponding signal region applies. The distribution of pseudo-$E_{\mathrm{T}}^{\mathrm{miss}}$ in the control regions is used to estimate the distribution of $E_{\mathrm{T}}^{\mathrm{miss}}$ expected from the $Z(\nu\nu) + \text{jets}$ and $\mathrm{W}(\ell\nu) + \text{jets}$ backgrounds in the signal region.

The dimuon control region is defined using the signal region selection criteria without the muon veto. Exactly two isolated muons with opposite charge, $p_{\mathrm{T}}^{\mu_1}$, $p_{\mathrm{T}}^{\mu_2} > 20, 10\,\mathrm{GeV}$ and an invariant mass in the range 60–120 GeV are required. As the decay branching fraction of $\mathcal{B}(Z \to \mu^+\mu^-)$ is approximately six times smaller than that to neutrinos, the resulting statistical uncertainty in the $\mathrm{Z}(\nu\nu) + \text{jets}$ background becomes a dominant systematic uncertainty at large values of $E_{\mathrm{T}}^{\mathrm{miss}}$. A complementary approach is to use events in data that have a high-p_{T} photon recoiling against jets to further constrain the $\mathrm{Z}(\nu\nu) + \text{jets}$ [83]. This is advantageous since the production cross section of $\gamma + \text{jets}$ is roughly a factor of three times that of the $\mathrm{Z}(\nu\nu) + \text{jets}$, yielding thereby a smaller statistical uncertainty in the predicted background. However, the theoretical uncertainties associated with the translation of the kinematics in $\gamma + \text{jets}$ events to that of $\mathrm{Z}(\nu\nu) + \text{jets}$ events are significant. A combination of both photon and dimuon control regions is used to maximally constrain the $\mathrm{Z}(\nu\nu) + \text{jets}$ background.

The photon control region consists of events that are selected by a trigger requiring an isolated photon with $p_{\mathrm{T}} > 150\,\mathrm{GeV}$ [70]. The selected events are required to have at least one photon with $p_{\mathrm{T}} > 170\,\mathrm{GeV}$ and $|\eta| < 2.5$, identified using a medium efficiency selection criterion [70]. Photons in the ECAL transition region, $1.44 < |\eta| < 1.56$ are excluded. All other kinematic selections are the same as those used for the signal region. The purity of the selection has been measured and is used to estimate the contributions from other backgrounds in the photon control region [70].

To estimate the $\mathrm{W}(\ell\nu) + \text{jets}$ background, a single muon control region is defined by selecting events with exactly one muon with $p_{\mathrm{T}} > 20\,\mathrm{GeV}$. Additionally, the transverse mass, calculated as $m_{\mathrm{T}} = \sqrt{2E_{\mathrm{T}}^{\mathrm{miss}} p_{\mathrm{T}}^{\mu}(1 - \cos\phi)}$, where ϕ is the azimuthal angle between $\vec{p}_{\mathrm{T}}^{\mathrm{miss}}$ and the direction of the muon momentum, is required to be in the range 50–100 GeV.

The $E_{\mathrm{T}}^{\mathrm{miss}}$ spectra of the $\mathrm{V} + \text{jets}$ backgrounds are determined through the use of a binned likelihood fit to the data in all the bins of the three control regions. The expected number of

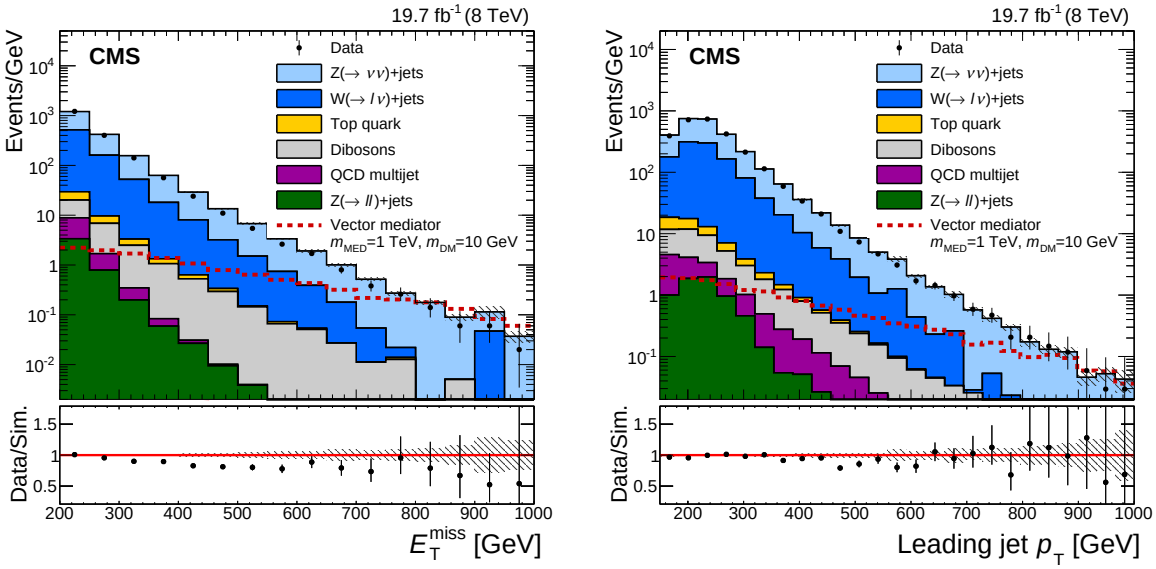

Figure 5: Distributions in $E_{\mathrm{T}}^{\mathrm{miss}}$ (left) and leading jet p_{T} (right) in simulated events and data, resulting from the combined signal selections for the three event categories. The dashed red line shows the expected distribution, assuming vector mediated DM production with $m_{\mathrm{MED}} = 1\,\mathrm{TeV}$ and $m_{\mathrm{DM}} = 10\,\mathrm{GeV}$. The shaded bands indicate the statistical uncertainty from the limited number of simulated events.

events N_i in a given bin i of pseudo-$E_{\mathrm{T}}^{\mathrm{miss}}$ is defined as $N_i^{\mathrm{Z}_{\mu\mu}} = \mu_i^{\mathrm{Z}\to\nu\nu}/R^{\mathrm{Z}}$ and $N_i^{\gamma} = \mu_i^{\mathrm{Z}\to\nu\nu}/R^{\gamma}$ for the dimuon and photon control regions, and $N_i^{\mathrm{W}} = \mu_i^{\mathrm{W}\to\ell\nu}/R_i^{\mathrm{W}}$ for the single muon control region. The $\mu_i^{\mathrm{Z}\to\nu\nu}$ and $\mu_i^{\mathrm{W}\to\ell\nu}$ terms are free parameters of the likelihood representing the yields of $\mathrm{Z}(\nu\nu)+\text{jets}$ and $\mathrm{W}(\ell\nu)+\text{jets}$ in each bin of the signal regions. The additional terms R_i^{W}, R_i^{Z}, and R_i^{γ} denote factors that account for the extrapolation of specific backgrounds from the signal region to control regions. The likelihood function for a particular event category is given by

$$\begin{aligned}\mathcal{L}(\boldsymbol{\mu}^{\mathrm{Z}\to\nu\nu},\boldsymbol{\mu}^{\mathrm{W}\to\ell\nu},\boldsymbol{\alpha},\boldsymbol{\beta}) = &\prod_i \mathrm{Poisson}\left(d_i^{\gamma}\middle|\left[B_i^{\gamma}(\boldsymbol{\alpha})+\frac{\mu_i^{\mathrm{Z}\to\nu\nu}}{R_i^{\gamma}(\boldsymbol{\beta})}\right]\right)\\ &\times\prod_i \mathrm{Poisson}\left(d_i^{\mathrm{Z}}\middle|\left[B_i^{\mathrm{Z}}(\boldsymbol{\alpha})+\frac{\mu_i^{\mathrm{Z}\to\nu\nu}}{R_i^{\mathrm{Z}}(\boldsymbol{\beta})}\right]\right)\\ &\times\prod_i \mathrm{Poisson}\left(d_i^{\mathrm{W}}\middle|\left[B_i^{\mathrm{W}}(\boldsymbol{\alpha})+\frac{\mu_i^{\mathrm{W}\to\ell\nu}}{R_i^{\mathrm{W}}(\boldsymbol{\beta})}\right]\right),\end{aligned} \tag{5}$$

where d_i^{γ}, d_i^{Z}, and d_i^{W} are the observed number of events in each bin, i, of the photon, dimuon, and single muon control regions and $\mathrm{Poisson}(x|y) = y^x\mathrm{e}^{-y}/x!$. The terms $\boldsymbol{\alpha},\boldsymbol{\beta}$ denote constrained nuisance parameters, which model systematic uncertainties in the translation from the pseudo-$E_{\mathrm{T}}^{\mathrm{miss}}$ distributions in the control regions of a particular event category to the $E_{\mathrm{T}}^{\mathrm{miss}}$ distribution in the corresponding signal region. The expected contributions from other background processes in the photon, dimuon and single muon control regions are denoted B_i^{γ}, B_i^{Z}, and B_i^{W} in Eq. (5), respectively.

The factors R_i^{Z} account for the ratio of $\mathcal{B}(\mathrm{Z}\to\nu\nu)/\mathcal{B}(\mathrm{Z}\to\mu^+\mu^-)$ and the muon efficiency times acceptance in the dimuon control region, while R_i^{γ} account for the ratio of differential cross sections between the $\mathrm{Z}+\text{jets}$ and $\gamma+\text{jets}$ processes and the efficiency times acceptance of the photon selection for the $\gamma+\text{jets}$ control region. The differential cross sections of photon

and Z production are corrected using NLO k-factors obtained from a comparison of their p_T distributions in events generated with MADGRAPH5_aMC@NLO 2.2.2 [66], to the distributions produced at LO. These k-factors are propagated to the factors R_i^γ to account for NLO QCD effects.

Systematic uncertainties are modelled as constrained nuisance parameters that allow variation of the factors R_i^γ, R_i^Z and R_i^W in the fit. These include theoretical uncertainties in the photon to Z differential cross section ratio from renormalization and factorization scale uncertainties, which amount to 8% each across the relevant boson p_T range. These uncertainties are conservative in that they are estimated by taking the maximum difference in the ratio derived from varying each scale by a factor of two, independently for the two processes, thereby ignoring any cancellation of the scale uncertainties. Electroweak corrections are not accounted for in the simulation. Additional k-factors are applied as a function of the boson (Z or γ) p_T, to account for higher order electroweak effects, which are around 15% for a boson p_T around 1 TeV [84]. The full correction is taken as an uncertainty in the ratio. A conservative choice is made in assuming this uncertainty to be uncorrelated across bins of E_T^{miss}. The uncertainties in the muon selection efficiency, photon selection efficiency, and photon purity are included and fully correlated across the control regions for the three event categories. The results of the fit to the data in the control regions for the V-boosted, V-resolved, and monojet categories are shown in Figs. 6, 7, and 8, respectively.

The remaining backgrounds are expected to be much smaller than those from V + jets and are estimated directly from simulation. Shape and normalization systematic uncertainties from the hadronic recoil corrections applied to these backgrounds are included and account for uncertainties in the jet energy scale and resolution. Systematic uncertainties related to the V-tagging efficiency of both of the V-tagged categories are included for the top and diboson backgrounds, which allow for migration of events between the three categories. The systematic uncertainty is roughly 10% in the V-resolved category, which allows for the disagreement between data and MC observed in the MVA distribution (Fig. 4) and 10% in the V-boosted category, which allows for the uncertainty in the measurement of the selection efficiency using ttbar events in data [78]. A systematic uncertainty of 4% is included for the top quark backgrounds normalization because of the uncertainty in the b tagging efficiency for the b jet veto in the V-resolved category [85]. Systematic uncertainties of 7% and 10% are included in the normalizations of the top quark [86] and diboson [87, 88] backgrounds, respectively, to account for the uncertainty in their cross sections in the relevant kinematic phase-space. The top quark and diboson backgrounds have been studied separately using dedicated control regions in data to validate these systematic uncertainties. A systematic uncertainty of 50% is included in the expected contribution from QCD multijet events. This uncertainty was obtained by taking the largest differences observed between data and simulation in events selected by inverting the requirement on $\Delta\phi(\vec{p}_T^{miss}, j)$. Finally, a systematic uncertainty of 2.6% in the integrated luminosity measurement [89] is included in the normalization all of the backgrounds obtained from simulation.

The expected yields in each bin of E_T^{miss} from all SM backgrounds, after the fit to the data in the control regions, are given in Tables 2, 3, and 4 for the V-boosted, V-resolved, and monojet signal region, respectively. The uncertainties represent the sum in quadrature of the effects of all the relevant sources of systematic uncertainty in each bin of E_T^{miss}. The correlations between the E_T^{miss} bins, resulting from the fit to the control regions, for each of the three event categories are shown in Figs. 12, 13, and 14 of the supplementary material in Appendix A.

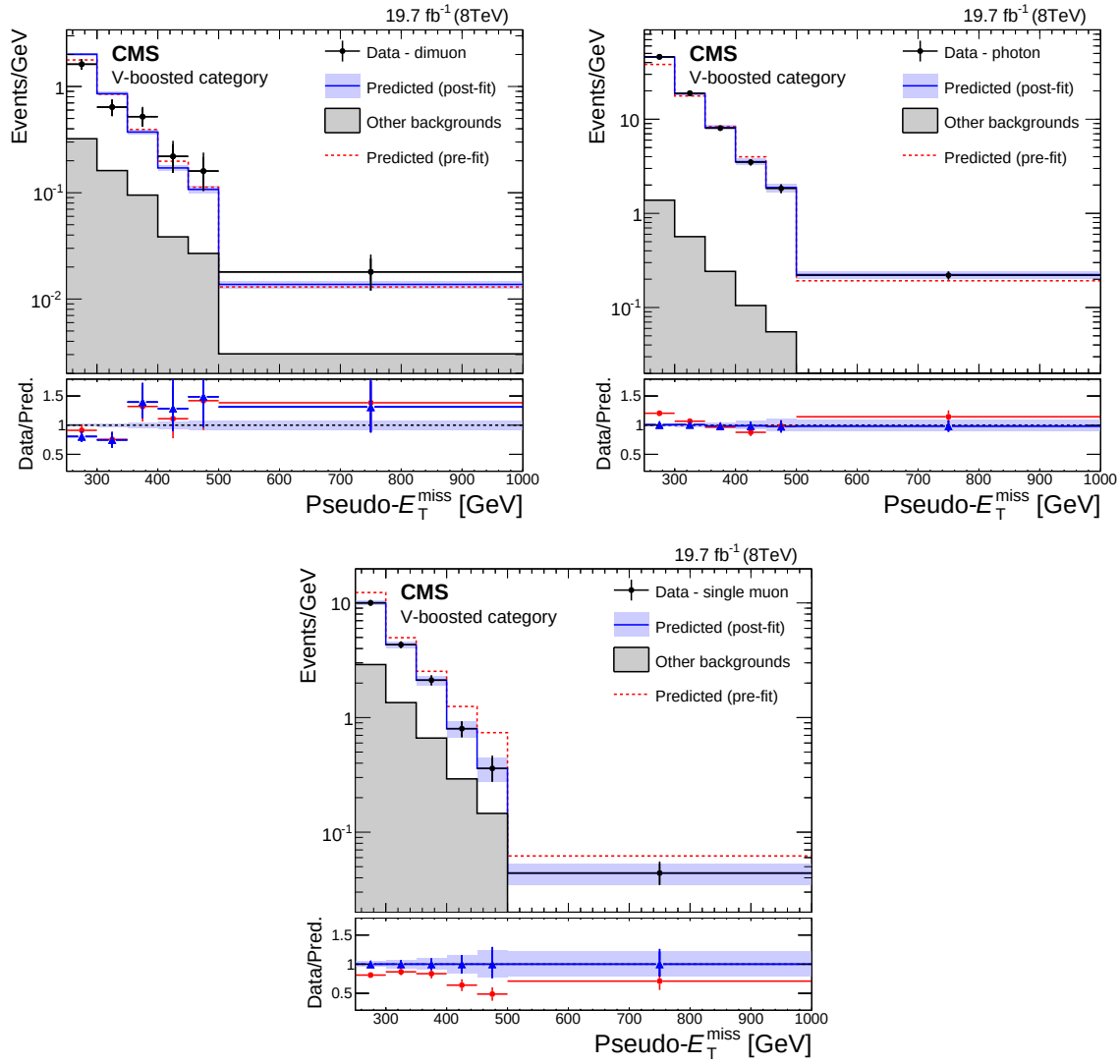

Figure 6: Predicted and observed pseudo-$E_{\mathrm{T}}^{\mathrm{miss}}$ distributions in the dimuon (top–left), photon (top–right), and single muon (bottom) control regions, before and after performing the simultaneous likelihood fit to the data in the control regions, for the V-boosted category. The predictions for the distributions before fitting to the control region data (pre-fit), and after (post-fit) are shown as the dashed red and solid blue lines, respectively. The red circles in the lower panels show the ratio of the observed data to the pre-fit predictions, while the blue triangles show the ratio to the post-fit predictions. The horizontal bars on the data points indicate the width of the bin that is centred at that point. The filled bands around the post-fit prediction indicate the combined statistical and systematic uncertainties from the fit.

Table 2: Expected yields of the SM processes and their uncertainties per bin for the V-boosted category after the fit to the control regions.

$E_{\mathrm{T}}^{\mathrm{miss}}$ (GeV)	Obs.	Z($\to \nu\nu$)+jets	W($\to \ell\nu$)+jets	Top quark	Dibosons	Other	Total Bkg.
250–300	1073	683±40	279±33	35.4±3.7	103±15	2.5±0.1	1103±63
300–350	453	271±23	114±20	12.7±1.3	46.5±6.9	0.7±0.1	446±34
350–400	160	118±13	38.3±8.7	5.6±1.0	22.2±3.3	0.2±0.1	184±18
400–450	81	49.7±7.3	9.8±3.4	1.5±0.8	11.0±1.8	<0.1	72±29
450–500	30	31.2±6.1	5.0±2.6	0.5±0.1	7.4±1.1	<0.1	44.3±6.6
500–1000	39	39.8±7.8	6.4±3.4	0.2±0.0	7.8±1.1	<0.1	54.3±8.5

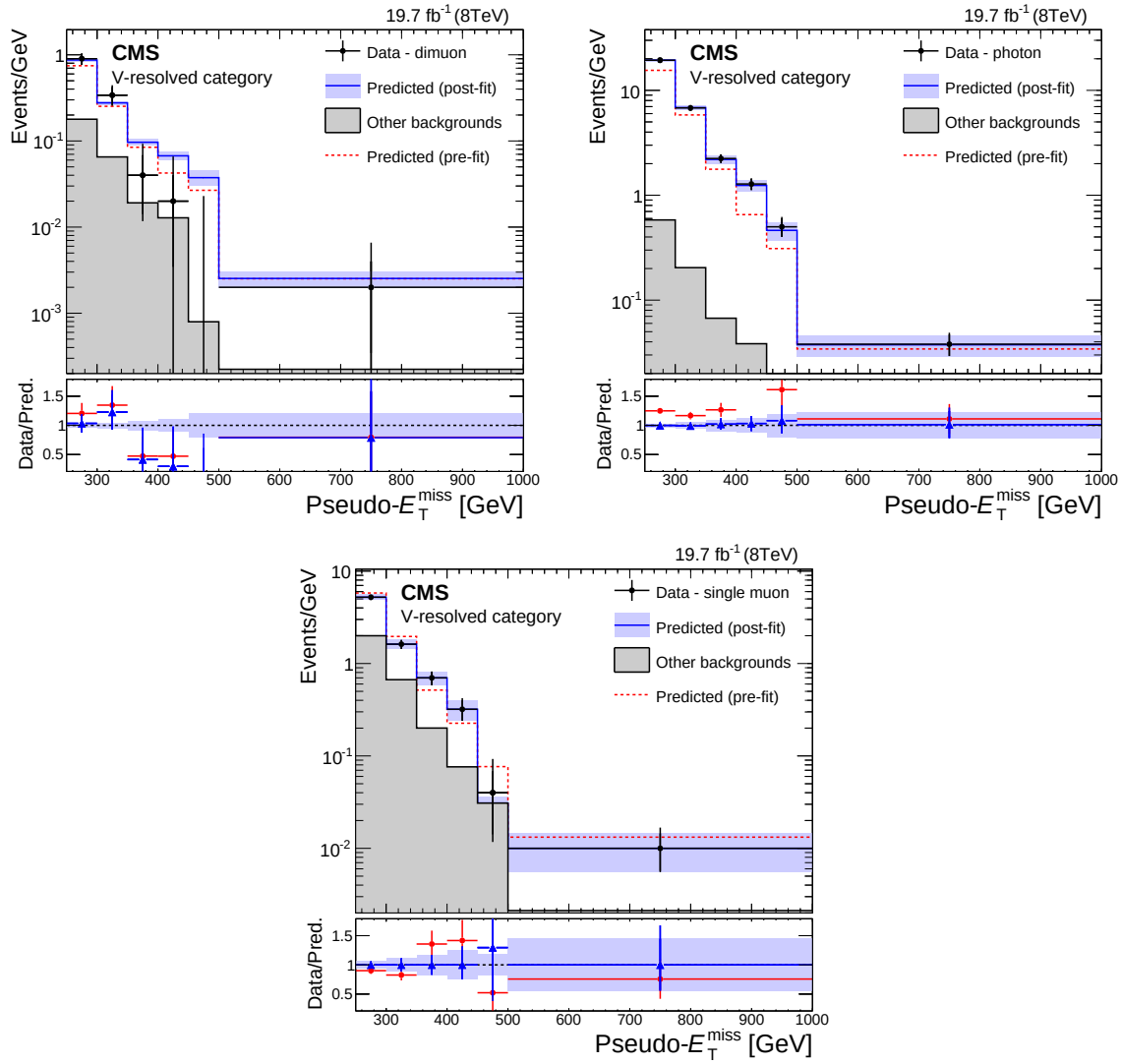

Figure 7: Predicted and observed pseudo-$E_{\mathrm{T}}^{\mathrm{miss}}$ distributions in the dimuon (top–left), photon (top–right), and single muon (bottom) control regions, before and after performing the simultaneous likelihood fit to the data in the control regions, for the V-resolved category. The predictions for the distributions before fitting to the control region data (pre-fit), and after (post-fit) are shown as the dashed red and solid blue lines, respectively. The red circles in the lower panels show the ratio of the observed data to the pre-fit predictions, while the blue triangles show the ratio to the post-fit predictions. The horizontal bars on the data points indicate the width of the bin that is centred at that point. The filled bands around the post-fit prediction indicate the combined statistical and systematic uncertainties from the fit.

Table 3: Expected yields of the SM processes and their uncertainties per bin for the V-resolved category after the fit to the control regions.

$E_{\mathrm{T}}^{\mathrm{miss}}$ (GeV)	Obs.	Z($\to \nu\nu$)+jets	W($\to \ell\nu$)+jets	Top quark	Dibosons	Other	Total Bkg.
250–300	617	298±36	166±26	55.4±4.7	27.9±1.6	36±17	587±48
300–350	211	98±14	41±10	15.2±1.5	9.6±0.3	19.2±6.6	170±18
350–400	79	31.1±7.0	21.5±8.9	5.5±0.7	3.2±0.3	8.2±2.3	62±12
400–450	20	20.1±6.4	14.5±8.5	1.5±0.2	0.6±0.3	3.0±0.7	38±11
450–500	16	6.1±2.7	1.0±2.6	1.0±0.4	0.4±0.1	1.0±0.2	8.5±3.6
500–1000	17	6.9±3.0	2.6±1.7	0.3±0.2	0.5±0.0	0.3±0.1	11.6±3.5

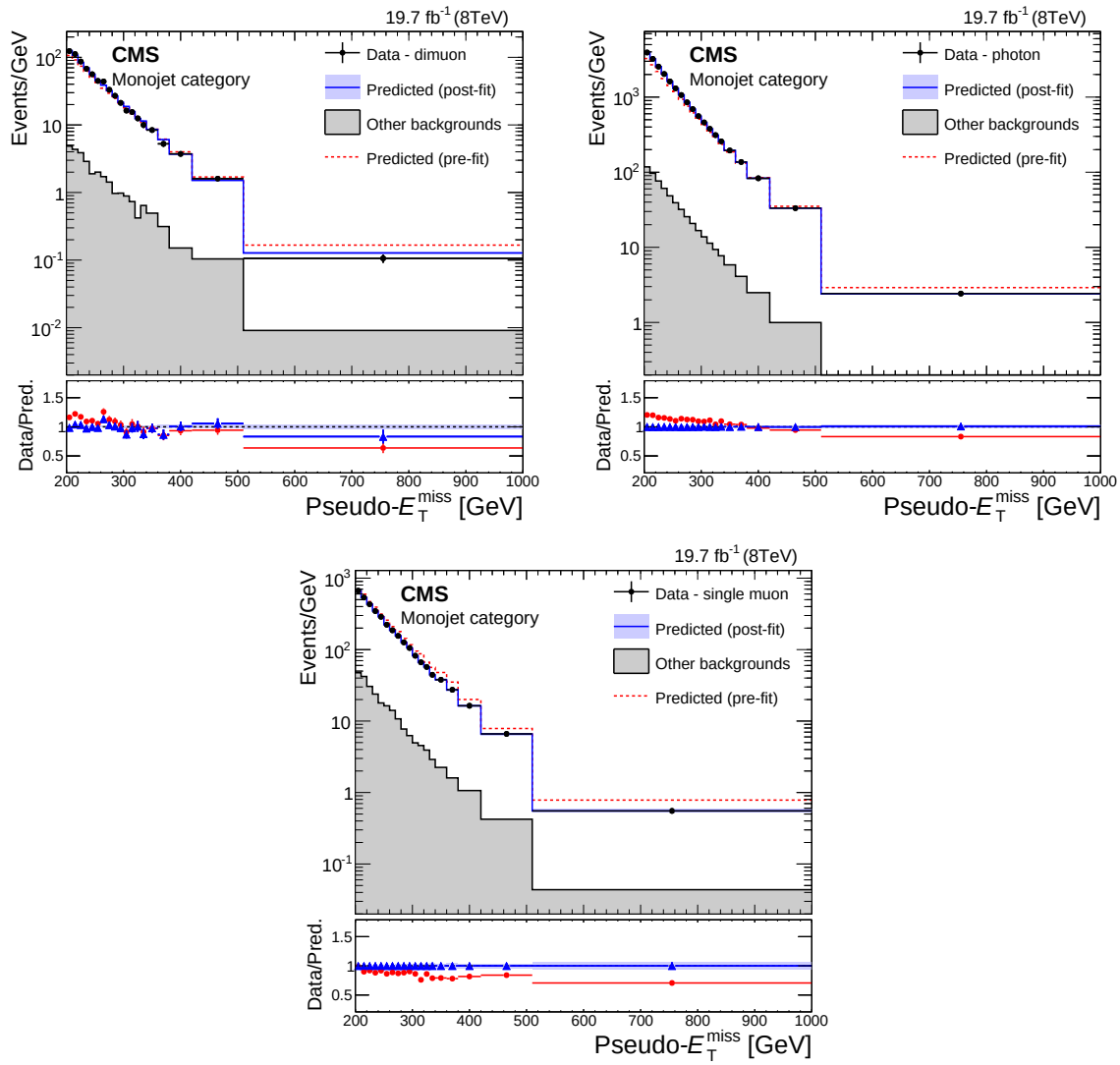

Figure 8: Predicted and observed pseudo-E_T^{miss} distributions in the dimuon (top–left), photon (top–right), and single muon (bottom) control regions, before and after performing the simultaneous likelihood fit to the data in the control regions, for the monojet category. The predictions for the distributions before fitting to the control region data (pre-fit), and after (post-fit) are shown as the dashed red and solid blue lines, respectively. The red circles in the lower panels show the ratio of the observed data to the pre-fit predictions, while the blue triangles show the ratio to the post-fit predictions. The horizontal bars on the data points indicate the width of the bin that is centred at that point. The filled bands around the post-fit prediction indicate the combined statistical and systematic uncertainties from the fit.

Table 4: Expected yields of the SM processes and their uncertainties per bin for the monojet category after the fit to the control regions.

$E_{\mathrm{T}}^{\mathrm{miss}}$ (GeV)	Obs.	Z($\to \nu\nu$)+jets	W($\to \ell\nu$)+jets	Top quark	Dibosons	Other	Total Bkg.
200–210	17547	10740±270	6770±320	132±11	135±14	93.4±16.9	17870±600
210–220	14303	9230±230	4990±240	104±13	112±11	63.7±6.7	14500±610
220–230	11343	7320±190	3830±170	82.1±7.3	95.1±9.6	39.4±2.4	11370±400
230–240	8961	5730±170	3020±160	62.0±5.8	77.9±8.6	29.0±1.0	8920±400
240–250	6920	4680±150	2470±140	46.6±4.4	61.0±6.1	19.6±0.5	7280±330
250–260	5582	3700±140	1860±120	34.2±3.7	50.1±4.9	14.6±0.4	5660±370
260–270	4517	3290±130	1580±110	27.7±2.3	39.7±4.2	10.3±0.2	4940±320
270–280	3693	2570±110	1101±71	25.0±3.1	33.5±3.4	6.3±0.2	3730±160
280–290	2907	2085±89	934±71	17.8±1.9	28.1±3.0	5.5±0.1	3070±180
290–300	2406	1721±85	754±58	15.0±3.6	21.9±2.7	4.2±0.1	2520±170
300–310	1902	1337±79	577±51	8.9±1.6	17.7±2.1	3.1±0.1	1940±160
310–320	1523	1182±58	435±43	5.9±2.2	15.5±1.8	2.3±0.1	1640±110
320–330	1316	931±53	371±44	5.2±1.3	11.0±1.8	2.1±0.1	1320±92
330–340	1065	804±51	246±29	4.9±1.1	11.9±1.8	1.8±0.1	1070±120
340–360	1571	1225±61	399±39	6.8±1.2	16.4±1.6	2.0±0.1	1650±110
360–380	1091	822±53	269±30	3.4±0.4	13.3±1.4	1.3±0.1	1110±150
380–420	1404	1036±66	324±30	5.5±0.6	17.1±1.7	1.4±0.1	1390±110
420–510	1126	943±70	267±27	3.9±0.8	15.7±1.6	1.3±0.1	1240±140
510–1000	476	330±32	72±12	0.6±0.2	8.2±0.8	0.3±0.1	412±71

6 Results

A simultaneous fit to the data in the three event category signal regions is performed. The background shapes in this second fit are allowed to vary within their uncertainties, which are propagated from the fit to the control region data, described in the previous section, accounting for correlations between the control region fit parameters. The corresponding comparisons between the data and the expected backgrounds in the $E_{\mathrm{T}}^{\mathrm{miss}}$ distributions after this fit are shown in Fig. 9 for each of the three event categories. Agreement between the data and the expected backgrounds is observed at the percent level across the three categories. A local significance of the data in each bin is calculated by comparing the likelihood between the background-only fit (Fig. 9) and a fit in which the total expected yield of events in that bin is fixed to the observation in data. The largest local significance observed using this procedure is 1.9 standard deviations and corresponds to the largest $E_{\mathrm{T}}^{\mathrm{miss}}$ bin of the monojet category.

The results are interpreted using the set of simplified models for DM production described in Section 3. Exclusion limits are set for these models using the asymptotic $\mathrm{CL_s}$ method [90–92] with a profile likelihood ratio as the test statistic, in which systematic uncertainties in the signal and background models are modelled as constrained nuisance parameters. For each signal hypothesis tested, upper limits are placed on the ratio of the signal yield to that predicted by the simplified model, denoted as μ. Limits are presented in terms of excluded regions in the $m_{\mathrm{MED}} - m_{\mathrm{DM}}$ plane, assuming scalar, pseudoscalar, vector, and axial-vector mediators, determined as the points for which $\mu > 1$ is excluded at the 90% confidence level (CL) or above. The choice of 90% CL exclusions is made to allow comparison with other experiments. Limits are calculated for a set of points in the plane and then interpolated to derive exclusion contours. In the region $m_{\mathrm{MED}} < 200\,\mathrm{GeV}$, $m_{\mathrm{DM}} < 200\,\mathrm{GeV}$, the limit is calculated in 10 GeV steps in both DM and mediator masses. For the region $200 < m_{\mathrm{MED}} < 500\,\mathrm{GeV}$, $m_{\mathrm{DM}} < 500\,\mathrm{GeV}$, a spacing of 25 GeV is used. For mediator masses larger than 500 GeV the generated signal points are separated by 100 GeV. The expected number of signal events in each of the three event categories arising from monojet and mono-V production for a vector and axial vector mediator with a

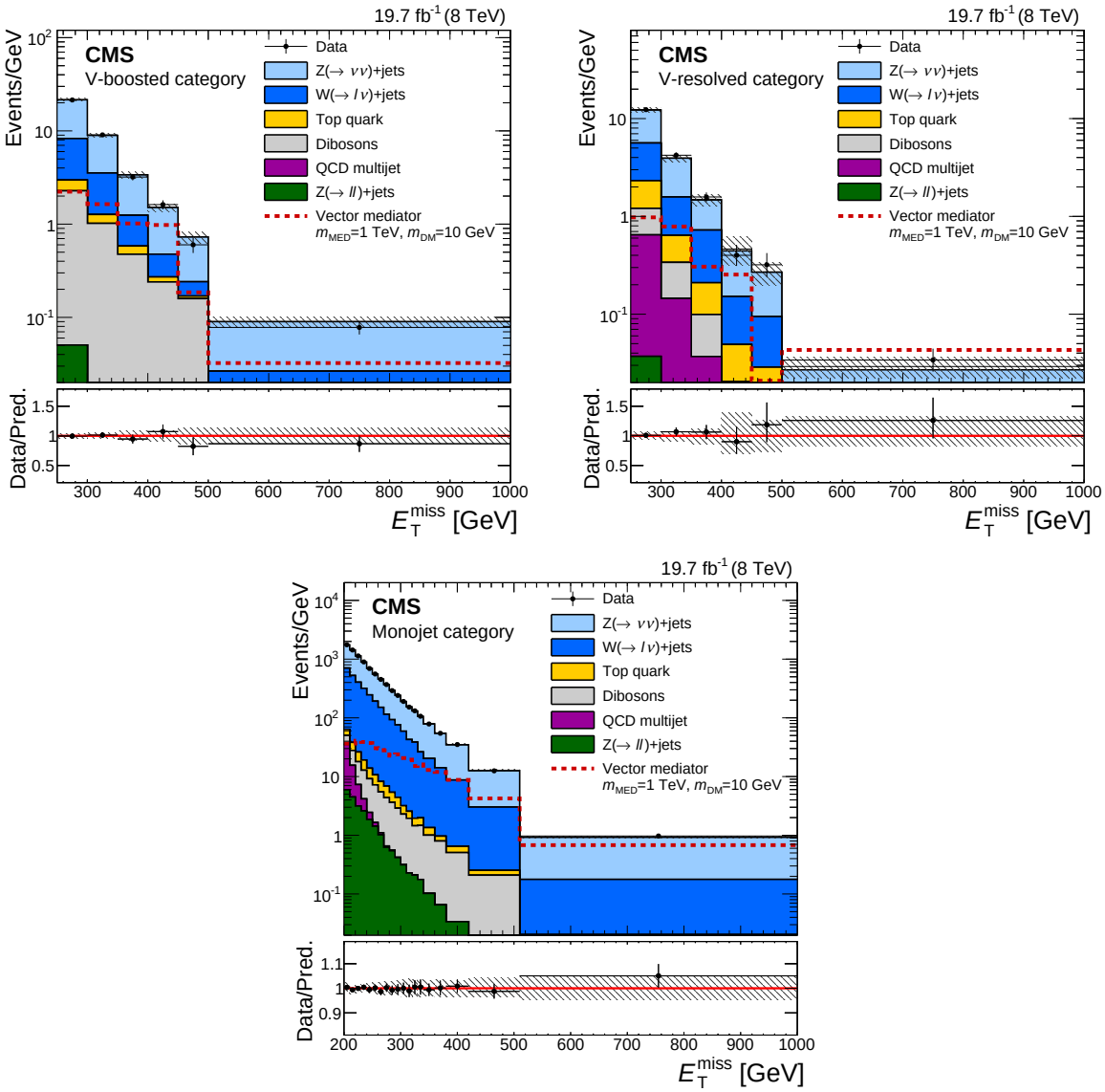

Figure 9: Post-fit distributions in $E_{\mathrm{T}}^{\mathrm{miss}}$ expected from SM backgrounds and observed in the signal region. The expected distributions are evaluated after fitting to the observed data simultaneously across the V-boosted (top–left), V-resolved (top–right), and monojet (bottom) categories. The ratio of the data to the post-fit background prediction is shown in the lower panels. The shaded bands indicate the post-fit uncertainty in the background, assuming no signal. The horizontal bars on the data points indicate the width of the bin that is centred at that point. The expected distribution for a signal assuming vector mediated DM production is shown for $m_{\mathrm{MED}} = 1\,\mathrm{TeV}$ and $m_{\mathrm{DM}} = 10\,\mathrm{GeV}$.

mass of 1 TeV, a scalar mediator with a mass of 125 GeV, and a pseudoscalar mediator with a mass of 400 GeV is shown in Table 5. The yields are derived assuming a DM mass of 1 GeV and coupling values $g_{\mathrm{DM}} = g_{\mathrm{SM}} = g_{\mathrm{q}} = 1$. The sum of these contributions in each category is used when setting limits, except in the fermionic case, for which the contribution from the mono-V signal is ignored.

Table 5: Expected signal event yields in each of the three event categories for monojet and mono-V production assuming a vector, axial vector, pseudoscalar, or scalar mediator. The yields are determined assuming $m_{\mathrm{DM}} = 1\,\mathrm{GeV}$ and $g_{\mathrm{DM}} = g_{\mathrm{SM}} = g_{\mathrm{q}} = 1$.

	V-boosted		V-resolved		Monojet	
Mediator type	monojet	mono-V	monojet	mono-V	monojet	mono-V
Vector, $m_{\mathrm{MED}} = 1\,\mathrm{TeV}$	217	84.0	82.0	26.1	5250	94.8
Axial vector, $m_{\mathrm{MED}} = 1\,\mathrm{TeV}$	268	85.7	85.5	24.5	6030	93.7
Pseudoscalar, $m_{\mathrm{MED}} = 400\,\mathrm{GeV}$	56.8	1300	20.8	100	2420	1500
Scalar, $m_{\mathrm{MED}} = 125\,\mathrm{GeV}$	20.6	126	8.44	13.3	1060	196

Experimental systematic uncertainties, including jet and $E_{\mathrm{T}}^{\mathrm{miss}}$ response and resolution uncertainties, are included in the signal model as nuisance parameters, while the theoretical systematic uncertainties in the inclusive cross section are instead added as additional contours on the exclusion limits. These include the effect of varying the renormalization and factorization scales by a factor of two, and the PDF uncertainties, which result in 20% and 30% variations in the signal yield, when summed in quadrature, for the vector and axial vector, and scalar and pseudoscalar models, respectively. These are the largest values found across the full range of the mediator mass from 10 GeV to 3 TeV, although the variation of these uncertainties in this range is found to be small. The same values are assumed for every signal point, thus giving a conservative estimate of the uncertainty.

Figure 10 shows the 90% CL exclusions for the vector, axial vector, scalar, and pseudoscalar mediator models. The 90% upper limit on μ (μ_{up}), when assuming that the mediator couples only to fermions (fermionic), is shown by the blue color scale. As described in Section 3, the limits are calculated assuming a minimum width for the signal [21, 22, 25, 93]. For the pseudoscalar interpretation, there is a region of masses between 150 and 280 GeV for which the decrease in cross section with larger mediator mass is balanced by an increase in acceptance for the signal, so that the expected signal contribution remains roughly constant. The expected value of μ_{up} is larger than 1 in this region, resulting in an "island" at small m_{DM}, where no exclusion is expected at the 90% CL. However, the observed value of μ_{up} is smaller than 1 throughout this region at 90% CL, thus the island is not present in the observed limits.

The results are compared, for all four types of mediators, to constraints obtained from the observed cosmological relic density of DM as determined from measurements of the cosmic microwave background by the WMAP and Planck experiments [5, 94, 95]. The expected DM abundance is estimated, separately for each model, using a thermal freeze-out mechanism implemented in MADDM2.0.6 [96], and compared with the observed cold DM density $\Omega_c h^2 = 0.12$ [97], as described in Ref. [98]. It is assumed that the hypothesized simplified model provides the only relevant dynamics for DM interaction beyond the SM.

Figures 11(top–left), 11(top–right), and 11(bottom–left) show the same exclusion contours, this time translated into the planes of $m_{\mathrm{DM}} - \sigma_{\mathrm{SI}}$ or $m_{\mathrm{DM}} - \sigma_{\mathrm{SD}}$, where σ_{SI} and σ_{SD} are the SI or SD DM-nucleon scattering cross sections. These representations allow a more direct comparison with limits from the DD experiments. The translations are obtained following the procedures outlined in Ref. [99] for the vector and axial vector mediators and in Refs. [100, 101] for the scalar mediator. It should be noted that the limits set from this analysis are only valid for

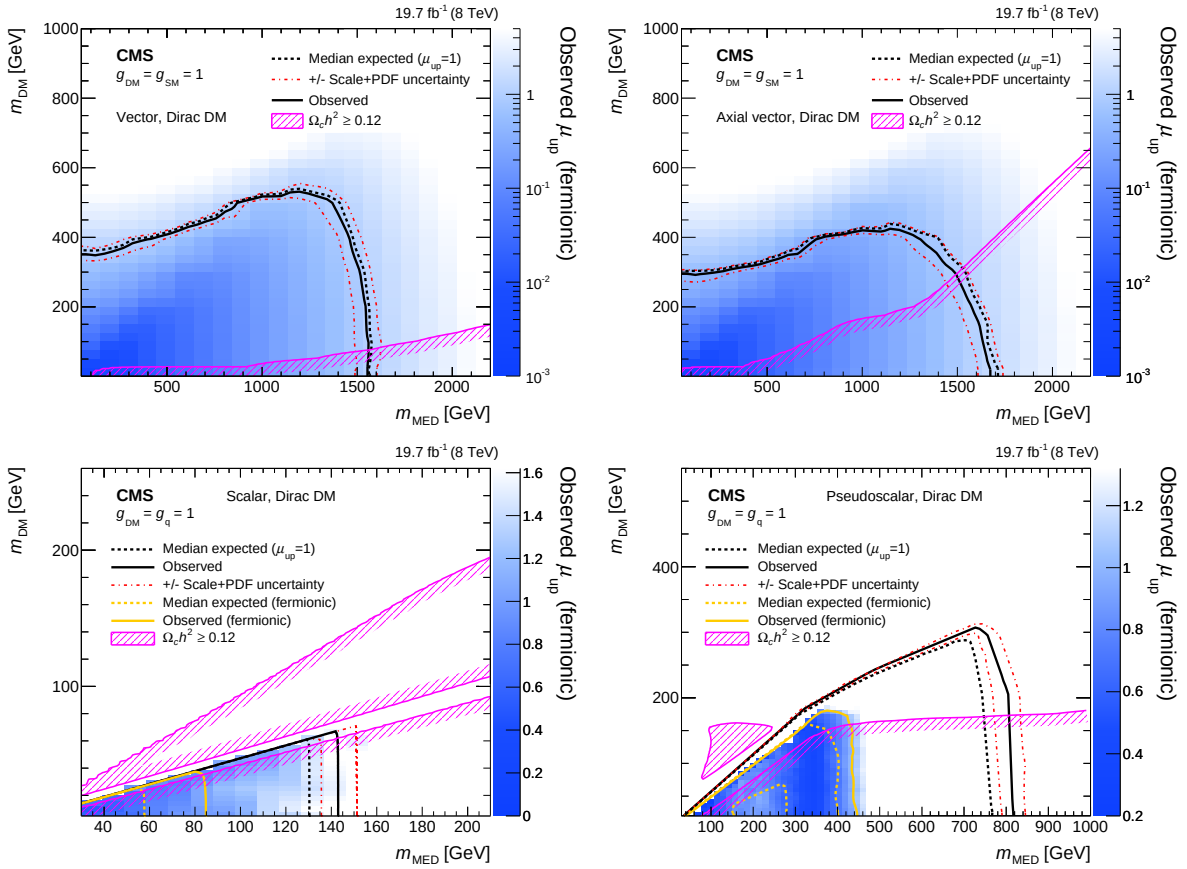

Figure 10: The 90% CL exclusion contours in the $m_{\mathrm{MED}} - m_{\mathrm{DM}}$ plane assuming vector (top–left), axial vector (top–right), scalar (bottom–left), and pseudoscalar (bottom–right) mediators. The scale shown on the right hand axis shows the expected 90% CL exclusion upper limit on the signal strength, assuming the mediator only couples to fermions. For the scalar and pseudoscalar mediators, the exclusion contour assuming coupling only to fermions (fermionic) is also shown. The white region shows model points that are not tested when assuming coupling only to fermions and are not expected to be excluded by this analysis under this assumption. The red dot-dashed lines indicate the variation in the exclusion contours due to modifying the renormalization and factorization scales by a factor of two in the generation of the signal. In all cases, the excluded region is to the bottom–left of the contours, except for the relic density, which shows the regions for which $\Omega_c h^2 \geq 0.12$, as indicated by the shading. In all of the models, the mediator width is determined using the minimum width assumption.

the simplified model, and in particular that they assume $g_{\mathrm{DM}} = g_{\mathrm{SM}} = g_{\mathrm{q}} = 1$. For the scalar mediator model, it is assumed that only heavy quarks (top and bottom) contribute. Such a choice limits the sensitivity for DD experiments, however, it allows the direct comparison between collider and DD experiments without an additional assumption for the light-quark couplings [100]. For the vector and scalar models, the limits are compared with those from the LUX [102], CDMS lite [103], CRESST II [104], and PandaX II [105] experiments. The limits from the LUX experiment currently provides the strongest constraints on σ_{SI} for $m_{\mathrm{DM}} \gtrsim 4\,\mathrm{GeV}$, while for values of $m_{\mathrm{DM}} < 2\,\mathrm{GeV}$ the analysis in this paper provides more stringent constraints on the vector and scalar models as shown in Figs. 11(top–left) and Fig. 11(bottom–left), respectively. For axial vector couplings, the limits are compared with DM–proton scattering limits from the PICO-2L [106], PICO-60 [107], IceCube [108], and Super-Kamiokande [109] experiments. In this model, the limits obtained in this analysis are superior for DM masses up to 300 GeV.

Pseudoscalar-mediated DM-nucleon interactions are suppressed at large velocities. The most appropriate comparison is therefore to the most sensitive bounds on indirect detection from the Fermi LAT collaboration [110, 111]. These limits apply to a scenario in which DM annihilates in the centre of a galaxy, producing a γ ray signature. The signature can be interpreted as DM annihilation to b quark pairs, allowing direct comparison with limits from this analysis [34, 112, 113].

Figure 11(bottom–right) shows the exclusion contours assuming pseudoscalar mediation in the plane of DM pair annihilation cross section versus m_{DM}. It is assumed that only heavy quarks contribute in the production of the mediator, while for the interpretation of the Fermi LAT limits in the annihilation cross section, it is assumed that the mediator decays only to b quark pairs. As with all of the simplified model interpretations, the DM particle is assumed to be a Dirac fermion. The results shown from Fermi LAT have been scaled by a factor of two compared to Ref. [110], because of the assumption of a Majorana DM fermion made by that analysis. The limits from this analysis improve on those from Fermi LAT for DM masses up to 150 GeV.

An excess in γ ray emission, consistent with the annihilation of DM, at the galactic centre has been reported in several studies using data from Fermi LAT [114–117]. Further studies of this excess suggest that DM annihilation could be mediated by a light pseudoscalar particle [118, 119]. The 68% CL preferred regions in this plane assuming the annihilation of DM pairs to light-quarks ($\mathrm{q\bar{q}}$), $\tau^+\tau^-$, or $\mathrm{b\bar{b}}$, using data from Fermi LAT, are shown as solid colour regions in Fig. 11(bottom–right). For the simplified model, and assuming that $g_{\mathrm{DM}} = g_{\mathrm{q}} = 1$, all of these regions are excluded by this analysis.

7 Summary

A search has been presented for an excess of events with at least one energetic jet in association with large $E_{\mathrm{T}}^{\mathrm{miss}}$ in a data sample of proton-proton collisions at a centre-of-mass energy of 8 TeV. The data correspond to an integrated luminosity of 19.7 fb^{-1} collected with the CMS detector at the LHC. Sensitivity to a potential mono-V signature is achieved by the addition of two event categories that select hadronically decaying V-bosons using novel jet substructure techniques. This search is the first at CMS to use jet substructure techniques to identify hadronically decaying vector bosons in both Lorentz-boosted and resolved scenarios. The sensitivity of the search has been increased compared to the previous CMS result by using the full shape of the $E_{\mathrm{T}}^{\mathrm{miss}}$ distribution to discriminate signal from standard model backgrounds and by using additional data control regions. No significant deviation is observed in the $E_{\mathrm{T}}^{\mathrm{miss}}$ distributions relative to the expectation from standard model backgrounds. The results of the search are interpreted under a set of simplified models that describe the production of dark matter (DM) particle pairs via vector, axial vector, scalar, or pseudoscalar mediation. Constraints are placed on the parameter space of these models. The search was the first at CMS to be interpreted using the simplified models for DM production. The search excludes DM production via vector or axial vector mediation with mediator masses up to 1.5 TeV, within the simplified model assumptions. When compared to direct detection experiments, the limits from this analysis provide the strongest constraints at small DM masses in the vector model and for DM masses up to 300 GeV in the axial vector model. For scalar and pseudoscalar mediated DM production, this analysis excludes mediator masses up to 80 and 400 GeV, respectively. The results of this analysis provide the strongest constraints on DM pair annihilation cross section via a pseudoscalar interaction for DM masses up to 150 GeV compared to the latest indirect detection results from Fermi LAT.

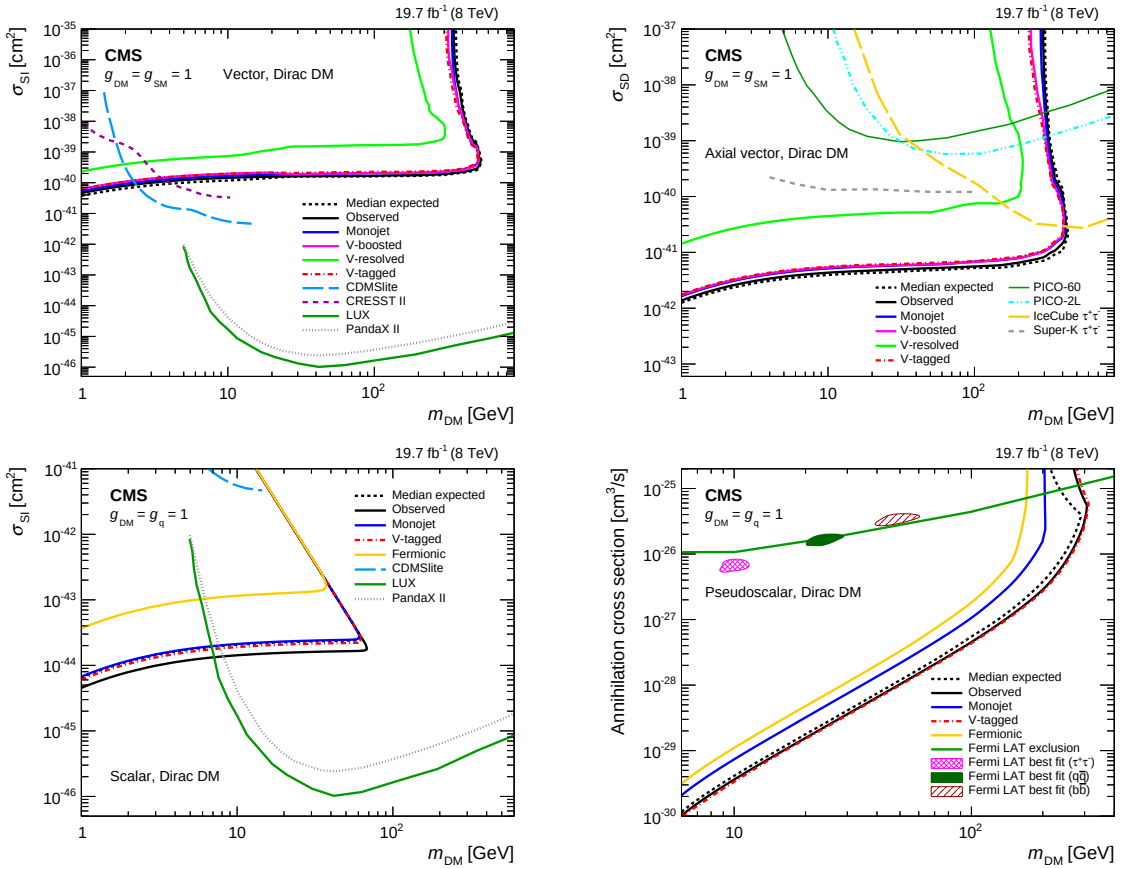

Figure 11: The 90% CL exclusion contours in the $m_{\mathrm{DM}} - \sigma_{\mathrm{SI}}$ or $m_{\mathrm{DM}} - \sigma_{\mathrm{SD}}$ plane assuming vector (top–left), axial vector (top–right), scalar (bottom–left) mediators. Also shown is the 90% CL exclusion in DM annihilation cross section as a function of m_{DM} for a pseudoscalar mediator (bottom–right). For the scalar and pseudoscalar mediators, the exclusion contours assuming the mediator only couples to fermions (fermionic) is also shown. The excluded region in all plots is to the top–left of the contours for the results from this analysis while the DD experiments and Fermi LAT excluded regions are above the lines shown. In the vector and axial vector models, limits are shown independently for monojet, V-boosted, and V-resolved categories. The red dot-dashed line shows the partial combination of the V-tagged categories for which the V-boosted category provides the dominant contribution. In all of the mediator models, a minimum mediator width is assumed. For the pseudoscalar mediator, 68% CL preferred regions, obtained using data from Fermi LAT, for DM annihilation to light-quarks ($q\bar{q}$), $\tau^+\tau^-$, and $b\bar{b}$ are given by the solid green, hatched pink, and shaded brown coloured regions, respectively.

Acknowledgments

We congratulate our colleagues in the CERN accelerator departments for the excellent performance of the LHC and thank the technical and administrative staffs at CERN and at other CMS institutes for their contributions to the success of the CMS effort. In addition, we gratefully acknowledge the computing centres and personnel of the Worldwide LHC Computing Grid for delivering so effectively the computing infrastructure essential to our analyses. Finally, we acknowledge the enduring support for the construction and operation of the LHC and the CMS detector provided by the following funding agencies: the Austrian Federal Ministry of Science, Research and Economy and the Austrian Science Fund; the Belgian Fonds de la Recherche Scientifique, and Fonds voor Wetenschappelijk Onderzoek; the Brazilian Funding Agencies (CNPq, CAPES, FAPERJ, and FAPESP); the Bulgarian Ministry of Education and Science; CERN; the Chinese Academy of Sciences, Ministry of Science and Technology, and National Natural Science Foundation of China; the Colombian Funding Agency (COLCIENCIAS); the Croatian Ministry of Science, Education and Sport, and the Croatian Science Foundation; the Research Promotion Foundation, Cyprus; the Secretariat for Higher Education, Science, Technology and Innovation, Ecuador; the Ministry of Education and Research, Estonian Research Council via IUT23-4 and IUT23-6 and European Regional Development Fund, Estonia; the Academy of Finland, Finnish Ministry of Education and Culture, and Helsinki Institute of Physics; the Institut National de Physique Nucléaire et de Physique des Particules / CNRS, and Commissariat à l'Énergie Atomique et aux Énergies Alternatives / CEA, France; the Bundesministerium für Bildung und Forschung, Deutsche Forschungsgemeinschaft, and Helmholtz-Gemeinschaft Deutscher Forschungszentren, Germany; the General Secretariat for Research and Technology, Greece; the National Scientific Research Foundation, and National Innovation Office, Hungary; the Department of Atomic Energy and the Department of Science and Technology, India; the Institute for Studies in Theoretical Physics and Mathematics, Iran; the Science Foundation, Ireland; the Istituto Nazionale di Fisica Nucleare, Italy; the Ministry of Science, ICT and Future Planning, and National Research Foundation (NRF), Republic of Korea; the Lithuanian Academy of Sciences; the Ministry of Education, and University of Malaya (Malaysia); the Mexican Funding Agencies (BUAP, CINVESTAV, CONACYT, LNS, SEP, and UASLP-FAI); the Ministry of Business, Innovation and Employment, New Zealand; the Pakistan Atomic Energy Commission; the Ministry of Science and Higher Education and the National Science Centre, Poland; the Fundação para a Ciência e a Tecnologia, Portugal; JINR, Dubna; the Ministry of Education and Science of the Russian Federation, the Federal Agency of Atomic Energy of the Russian Federation, Russian Academy of Sciences, and the Russian Foundation for Basic Research; the Ministry of Education, Science and Technological Development of Serbia; the Secretaría de Estado de Investigación, Desarrollo e Innovación and Programa Consolider-Ingenio 2010, Spain; the Swiss Funding Agencies (ETH Board, ETH Zurich, PSI, SNF, UniZH, Canton Zurich, and SER); the Ministry of Science and Technology, Taipei; the Thailand Center of Excellence in Physics, the Institute for the Promotion of Teaching Science and Technology of Thailand, Special Task Force for Activating Research and the National Science and Technology Development Agency of Thailand; the Scientific and Technical Research Council of Turkey, and Turkish Atomic Energy Authority; the National Academy of Sciences of Ukraine, and State Fund for Fundamental Researches, Ukraine; the Science and Technology Facilities Council, UK; the US Department of Energy, and the US National Science Foundation.

Individuals have received support from the Marie-Curie programme and the European Research Council and EPLANET (European Union); the Leventis Foundation; the A. P. Sloan Foundation; the Alexander von Humboldt Foundation; the Belgian Federal Science Policy Office; the Fonds pour la Formation à la Recherche dans l'Industrie et dans l'Agriculture (FRIA-

Belgium); the Agentschap voor Innovatie door Wetenschap en Technologie (IWT-Belgium); the Ministry of Education, Youth and Sports (MEYS) of the Czech Republic; the Council of Science and Industrial Research, India; the HOMING PLUS programme of the Foundation for Polish Science, cofinanced from European Union, Regional Development Fund, the Mobility Plus programme of the Ministry of Science and Higher Education, the National Science Center (Poland), contracts Harmonia 2014/14/M/ST2/00428, Opus 2013/11/B/ST2/04202, 2014/13/B/ST2/02543 and 2014/15/B/ST2/03998, Sonata-bis 2012/07/E/ST2/01406; the Thalis and Aristeia programmes cofinanced by EU-ESF and the Greek NSRF; the National Priorities Research Program by Qatar National Research Fund; the Programa Clarín-COFUND del Principado de Asturias; the Rachadapisek Sompot Fund for Postdoctoral Fellowship, Chulalongkorn University and the Chulalongkorn Academic into Its 2nd Century Project Advancement Project (Thailand); and the Welch Foundation, contract C-1845.

References

[1] H. C. van de Hulst, E. Raimond, and H. van Woerden, "Rotation and density distribution of the Andromeda nebula derived from observations of the 21-cm line", *Bull. Astr. Inst. Netherlands* **14** (1957) 1.

[2] V. C. Rubin, N. Thonnard, and W. K. Ford Jr., "Rotational properties of 21 SC galaxies with a large range of luminosities and radii, from NGC 4605/R = 4 kpc to UGC 2885/R = 122 kpc", *Astrophys. J.* **238** (1980) 471, doi:10.1086/158003.

[3] G. F. Smoot et al., "Structure in the COBE differential microwave radiometer first year maps", *Astrophys. J.* **396** (1992) L1, doi:10.1086/186504.

[4] Boomerang Collaboration, "A flat Universe from high resolution maps of the cosmic microwave background radiation", *Nature* **404** (2000) 955, doi:10.1038/35010035, arXiv:astro-ph/0004404.

[5] WMAP Collaboration, "Wilkinson microwave anisotropy probe (WMAP) three year results: implications for cosmology", *Astrophys. J. Suppl.* **170** (2007) 377, doi:10.1086/513700, arXiv:astro-ph/0603449.

[6] J. L. Feng, "Dark matter candidates from particle physics and methods of detection", *Ann. Rev. Astron. Astrophys.* **48** (2010) 495, doi:10.1146/annurev-astro-082708-101659, arXiv:1003.0904.

[7] T. A. Porter, R. P. Johnson, and P. W. Graham, "Dark matter searches with astroparticle data", *Ann. Rev. Astron. Astrophys.* **49** (2011) 155, doi:10.1146/annurev-astro-081710-102528, arXiv:1104.2836.

[8] ATLAS Collaboration, "Search for new phenomena in final states with an energetic jet and large missing transverse momentum in pp collisions at $\sqrt{s} = 13$ TeV using the ATLAS detector", *Phys. Rev. D* **94** (Aug, 2016) 032005, doi:10.1103/PhysRevD.94.032005.

[9] CMS Collaboration, "Search for dark matter, extra dimensions, and unparticles in monojet events in proton proton collisions at $\sqrt{s} = 8$ TeV", *Eur. Phys. J. C* **75** (2015) 235, doi:10.1140/epjc/s10052-015-3451-4, arXiv:1408.3583.

[10] ATLAS Collaboration, "Search for new phenomena in final states with an energetic jet and large missing transverse momentum in pp collisions at $\sqrt{s} = 8$ TeV with the ATLAS detector", *Eur. Phys. J. C* **75** (2015) 299, doi:10.1140/epjc/s10052-015-3517-3, arXiv:1502.01518. [Erratum: doi:10.1140/epjc/s10052-015-3639-7].

[11] ATLAS Collaboration, "Search for dark matter candidates and large extra dimensions in events with a jet and missing transverse momentum with the ATLAS detector", *JHEP* **04** (2013) 075, doi:10.1007/JHEP04(2013)075, arXiv:1210.4491.

[12] ATLAS Collaboration, "Search for new phenomena with the monojet and missing transverse momentum signature using the ATLAS detector in $\sqrt{s} = 7$ TeV proton-proton collisions", *Phys. Lett. B* **705** (2011) 294, doi:10.1016/j.physletb.2011.10.006, arXiv:1106.5327.

[13] CMS Collaboration, "Search for dark matter and large extra dimensions in monojet events in pp collisions at $\sqrt{s} = 7$ TeV", *JHEP* **09** (2012) 094, doi:10.1007/JHEP09(2012)094, arXiv:1206.5663.

[14] CMS Collaboration, "Search for dark matter particles in proton-proton collisions at $\sqrt{s}$ = 8 TeV using the razor variables", (2016). arXiv:1603.08914. Submitted to *JHEP*.

[15] CMS Collaboration, "Search for physics beyond the standard model in final states with a lepton and missing transverse energy in proton-proton collisions at $\sqrt{s}$ = 8 TeV", *Phys. Rev. D* **91** (2015) 092005, doi:10.1103/PhysRevD.91.092005, arXiv:1408.2745.

[16] ATLAS Collaboration, "Search for dark matter in events with a Z boson and missing transverse momentum in pp collisions at $\sqrt{s}$ = 8 TeV with the ATLAS detector", *Phys. Rev. D* **90** (2014) 012004, doi:10.1103/PhysRevD.90.012004, arXiv:1404.0051.

[17] ATLAS Collaboration, "Search for dark matter in events with a hadronically decaying W or Z boson and missing transverse momentum in pp collisions at $\sqrt{s} = 8$ TeV with the ATLAS detector", *Phys. Rev. Lett.* **112** (2014) 041802, doi:10.1103/PhysRevLett.112.041802, arXiv:1309.4017.

[18] ATLAS Collaboration, "Search for new particles in events with one lepton and missing transverse momentum in pp collisions at $\sqrt{s}$ = 8 TeV with the ATLAS detector", *JHEP* **09** (2014) 037, doi:10.1007/JHEP09(2014)037, arXiv:1407.7494.

[19] M. Beltran et al., "Maverick dark matter at colliders", *JHEP* **09** (2010) 37, doi:10.1007/JHEP09(2010)037, arXiv:1002.4137.

[20] J. Goodman et al., "Constraints on dark matter from colliders", *Phys. Rev. D* **82** (2010) 116010, doi:10.1103/PhysRevD.82.116010, arXiv:1008.1783.

[21] P. J. Fox, R. Harnik, J. Kopp, and Y. Tsai, "Missing energy signatures of dark matter at the LHC", *Phys. Rev. D* **85** (2012) 056011, doi:10.1103/PhysRevD.85.056011, arXiv:1109.4398.

[22] G. Busoni, A. D. Simone, E. Morgante, and A. Riotto, "On the validity of the effective field theory for dark matter searches at the LHC", *Phys. Lett. B* **728C** (2014) 412., doi:10.1016/j.physletb.2013.11.069, arXiv:1307.2253.

[23] O. Buchmueller, M. J. Dolan, and C. McCabe, "Beyond effective field theory for dark matter searches at the LHC", *JHEP* **01** (2014) 025, doi:10.1007/JHEP01(2014)025, arXiv:1308.6799.

[24] O. Buchmueller, M. J. Dolan, S. A. Malik, and C. McCabe, "Characterising dark matter searches at colliders and direct detection experiments: Vector mediators", *JHEP* **01** (2015) 037, doi:10.1007/JHEP01(2015)037, arXiv:1407.8257.

[25] D. Abercrombie et al., "Dark matter benchmark models for early LHC Run-2 searches: Report of the ATLAS/CMS Dark Matter Forum", (2015). arXiv:1507.00966.

[26] CMS Collaboration, "The CMS experiment at the CERN LHC", *JINST* **3** (2008) S08004, doi:10.1088/1748-0221/3/08/S08004.

[27] CMS Collaboration, "Particle–Flow Event Reconstruction in CMS and Performance for Jets, Taus, and $E_{\mathrm{T}}^{\mathrm{miss}}$", CMS Physics Analysis Summary CMS-PAS-PFT-09-001, 2009.

[28] CMS Collaboration, "Commissioning of the Particle-flow Event Reconstruction with the first LHC collisions recorded in the CMS detector", CMS Physics Analysis Summary CMS-PAS-PFT-10-001, 2010.

[29] M. Cacciari, G. P. Salam, and G. Soyez, "The anti-k_t jet clustering algorithm", *JHEP* **04** (2008) 063, doi:10.1088/1126-6708/2008/04/063, arXiv:0802.1189.

[30] CMS Collaboration, "A Cambridge-Aachen (C-A) based jet algorithm for boosted top-jet tagging", CMS Physics Analysis Summary CMS-PAS-JME-09-001, 2009.

[31] CMS Collaboration, "Determination of jet energy calibration and transverse momentum resolution in CMS", *J. Instrum.* **6** (2011) P11002, doi:10.1088/1748-0221/6/11/P11002.

[32] M. Cacciari, G. P. Salam, and G. Soyez, "FastJet user manual", *Eur. Phys. J. C* **72** (2012) 1896, doi:10.1140/epjc/s10052-012-1896-2, arXiv:1111.6097.

[33] CMS Collaboration, "Performance of the CMS missing transverse momentum reconstruction in pp data at $\sqrt{s}$ = 8 TeV", *JINST* **10** (2015) P02006, doi:10.1088/1748-0221/10/02/P02006, arXiv:1411.0511.

[34] P. Harris, V. V. Khoze, M. Spannowsky, and C. Williams, "Constraining dark sectors at colliders: beyond the effective theory approach", *Phys. Rev. D* **91** (2015) 055009, doi:10.1103/PhysRevD.91.055009, arXiv:1411.0535.

[35] U. Haisch, F. Kahlhoefer, and J. Unwin, "The impact of heavy-quark loops on LHC dark matter searches", *JHEP* **07** (2013) 125, doi:10.1007/JHEP07(2013)125, arXiv:1208.4605.

[36] L. Lopez-Honorez, T. Schwetz, and J. Zupan, "Higgs portal, fermionic dark matter, and a Standard Model like Higgs at 125 GeV", *Phys. Lett. B* **716** (2012) 179, doi:10.1016/j.physletb.2012.07.017, arXiv:1203.2064.

[37] M. Chala et al., "Constraining dark sectors with monojets and dijets", *JHEP* **07** (2015) 089, doi:10.1007/JHEP07(2015)089, arXiv:1503.05916.

[38] A. Alves, S. Profumo, and F. S. Queiroz, "The dark Z' portal: direct, indirect and collider searches", *JHEP* **04** (2014) 063, doi:10.1007/JHEP04(2014)063, arXiv:1312.5281.

[39] G. Arcadi, Y. Mambrini, M. H. G. Tytgat, and B. Zaldivar, "Invisible Z' and dark matter: LHC vs LUX constraints", *JHEP* **03** (2014) 134, doi:10.1007/JHEP03(2014)134, arXiv:1401.0221.

[40] ATLAS Collaboration, "Search for new phenomena in dijet mass and angular distributions from pp collisions at $\sqrt{s} = 13$ TeV with the ATLAS detector", *Phys. Lett. B* **754** (2016) 302, doi:10.1016/j.physletb.2016.01.032, arXiv:1512.01530.

[41] ATLAS Collaboration, "Search for new phenomena in the dijet mass distribution using pp collision data at $\sqrt{s} = 8$ TeV with the ATLAS detector", *Phys. Rev. D* **91** (2015), no. 5, 052007, doi:10.1103/PhysRevD.91.052007, arXiv:1407.1376.

[42] CMS Collaboration, "Search for resonances and quantum black holes using dijet mass spectra in proton-proton collisions at $\sqrt{s} = 8$ TeV", *Phys. Rev. D* **91** (2015), no. 5, 052009, doi:10.1103/PhysRevD.91.052009, arXiv:1501.04198.

[43] V. V. Khoze, G. Ro, and M. Spannowsky, "Spectroscopy of scalar mediators to dark matter at the LHC and at 100 TeV", *Phys. Rev. D* **92** (2015) 075006, doi:10.1103/PhysRevD.92.075006, arXiv:1505.03019.

[44] T. Hambye and A. Strumia, "Dynamical generation of the weak and dark matter scale", *Phys. Rev. D* **88** (2013) 055022, doi:10.1103/PhysRevD.88.055022, arXiv:1306.2329.

[45] V. V. Khoze, C. McCabe, and G. Ro, "Higgs vacuum stability from the dark matter portal", *JHEP* **08** (2014) 026, doi:10.1007/JHEP08(2014)026, arXiv:1403.4953.

[46] V. V. Khoze and G. Ro, "Dark matter monopoles, vectors and photons", *JHEP* **10** (2014) 61, doi:10.1007/JHEP10(2014)061, arXiv:1406.2291.

[47] W. Altmannshofer et al., "Light dark matter, naturalness, and the radiative origin of the electroweak scale", *JHEP* **01** (2015) 032, doi:10.1007/JHEP01(2015)032, arXiv:1408.3429.

[48] C. D. Carone and R. Ramos, "Classical scale-invariance, the electroweak scale and vector dark matter", *Phys. Rev. D* **88** (2013) 055020, doi:10.1103/PhysRevD.88.055020, arXiv:1307.8428.

[49] M. Heikinheimo et al., "Physical naturalness and dynamical breaking of classical scale invariance", *Mod. Phys. Lett. A* **29** (2014) 1450077, doi:10.1142/S0217732314500771, arXiv:1304.7006.

[50] J. M. Campbell and R. K. Ellis, "MCFM for the Tevatron and the LHC", *Nucl. Phys. Proc. Suppl.* **205-206** (2010) 10, doi:10.1016/j.nuclphysbps.2010.08.011, arXiv:1007.3492.

[51] I. Anderson et al., "Constraining anomalous HVV interactions at proton and lepton colliders", *Phys. Rev. D* **89** (2014) 035007, doi:10.1103/PhysRevD.89.035007, arXiv:1309.4819.

[52] R. V. Harlander, T. Neumann, K. J. Ozeren, and M. Wiesemann, "Top-mass effects in differential Higgs production through gluon fusion at order α_s^4", *JHEP* **08** (2012) 139, doi:10.1007/JHEP08(2012)139, arXiv:1206.0157.

[53] T. Neumann and M. Wiesemann, "Finite top-mass effects in gluon-induced Higgs production with a jet-veto at NNLO", *JHEP* **11** (2014) 150, doi:10.1007/JHEP11(2014)150, arXiv:1408.6836.

[54] NNPDF Collaboration, "Parton distributions for the LHC Run II", *JHEP* **04** (2015) 040, doi:10.1007/JHEP04(2015)040, arXiv:1410.8849.

[55] T. Sjöstrand, S. Mrenna, and P. Z. Skands, "PYTHIA 6.4 physics and manual", *JHEP* **05** (2006) 026, doi:10.1088/1126-6708/2006/05/026, arXiv:hep-ph/0603175.

[56] CMS Collaboration, "Jet and underlying event properties as a function of charged-particle multiplicity in proton-proton collisions at $\sqrt{s} = 7$ TeV", *Eur. Phys. J. C* **73** (2013), no. 12, 2674, doi:10.1140/epjc/s10052-013-2674-5, arXiv:1310.4554.

[57] P. Nason, "A mew method for combining NLO QCD with shower Monte Carlo algorithms", *JHEP* **11** (2004) 040, doi:10.1088/1126-6708/2004/11/040, arXiv:hep-ph/0409146.

[58] S. Frixione, P. Nason, and C. Oleari, "Matching NLO QCD computations with parton shower simulations: the POWHEG method", *JHEP* **11** (2007) 070, doi:10.1088/1126-6708/2007/11/070, arXiv:0709.2092.

[59] C. Oleari, "The POWHEG BOX", *Nuc. Phys. B Proc. Sup.* **205** (2010) 36, doi:10.1016/j.nuclphysbps.2010.08.016, arXiv:1007.3893.

[60] S. Alioli, P. Nason, C. Oleari, and E. Re, "A general framework for implementing NLO calculations in shower Monte Carlo programs: the POWHEG BOX", *JHEP* **06** (2010) 043, doi:10.1007/JHEP06(2010)043, arXiv:1002.2581.

[61] S. Alioli, P. Nason, C. Oleari, and E. Re, "NLO single-top production matched with shower in POWHEG: s- and t-channel contributions", *JHEP* **09** (2009) 111, doi:10.1088/1126-6708/2009/09/111, arXiv:0907.4076. [Erratum: doi:10.1007/JHEP02(2010)011].

[62] T. Sjöstrand, S. Mrenna, and P. Z. Skands, "A brief introduction to PYTHIA 8.1", *Comput. Phys. Commun.* **178** (2008) 852, doi:10.1016/j.cpc.2008.01.036, arXiv:0710.3820.

[63] CMS Collaboration, "Event generator tunes obtained from underlying event and multiparton scattering measurements", *Eur. Phys. J. C* **76** (2016) 155, doi:10.1140/epjc/s10052-016-3988-x, arXiv:1512.00815.

[64] A. Denner, S. Dittmaier, S. Kallweit, and A. Muck, "Electroweak corrections to Higgs-strahlung off W/Z bosons at the Tevatron and the LHC with HAWK", *JHEP* **03** (2012) 075, doi:10.1007/JHEP03(2012)075, arXiv:1112.5142.

[65] O. Brein, A. Djouadi, and R. Harlander, "NNLO QCD corrections to the Higgs-strahlung processes at hadron colliders", *Phys. Lett. B* **579** (2004) 149, doi:10.1016/j.physletb.2003.10.112, arXiv:hep-ph/0307206.

[66] J. Alwall et al., "The automated computation of tree-level and next-to-leading order differential cross sections, and their matching to parton shower simulations", *JHEP* **07** (2014) 079, doi:10.1007/JHEP07(2014)079, arXiv:1405.0301.

[67] M. L. Mangano, M. Moretti, F. Piccinini, and M. Treccani, "Matching matrix elements and shower evolution for top-quark production in hadronic collisions", *JHEP* **01** (2007) 013, doi:10.1088/1126-6708/2007/01/013, arXiv:hep-ph/0611129.

[68] J. Gao et al., "CT10 next-to-next-to-leading order global analysis of QCD", *Phys. Rev. D* **89** (2014) 033009, doi:10.1103/PhysRevD.89.033009, arXiv:1302.6246.

[69] GEANT4 Collaboration, "GEANT4—a simulation toolkit", *Nucl. Instrum. Meth. A* **506** (2003) 250, doi:10.1016/S0168-9002(03)01368-8.

[70] CMS Collaboration, "Performance of photon reconstruction and identification with the CMS detector in proton-proton collisions at $\sqrt{s}$ = 8 TeV", *JINST* **10** (2015) P08010, doi:10.1088/1748-0221/10/08/P08010, arXiv:1502.02702.

[71] CMS Collaboration, "Performance of electron reconstruction and selection with the CMS Detector in proton-proton collisions at $\sqrt{s} = 8$ TeV", *JINST* **10** (2015) P06005, doi:10.1088/1748-0221/10/06/P06005, arXiv:1502.02701.

[72] CMS Collaboration, "Reconstruction and identification of tau lepton decays to hadrons and tau neutrinos at CMS", *JINST* **11** (2016) P01019, doi:10.1088/1748-0221/11/01/P01019, arXiv:1510.07488.

[73] CMS Collaboration, "The performance of the CMS muon detector in proton-proton collisions at sqrt(s) = 7 TeV at the LHC", *JINST* **8** (2013) P11002, doi:10.1088/1748-0221/8/11/P11002, arXiv:1306.6905.

[74] CMS Collaboration, "The CMS Particle Flow Algorithm", in *Proceedings, International Conference on Calorimetry for the High Energy Frontier (CHEF 2013)*, p. 295. 2013. arXiv:1401.8155.

[75] J. Thaler and K. Van Tilburg, "Identifying boosted objects with N-subjettiness", *JHEP* **03** (2011) 015, doi:10.1007/JHEP03(2011)015, arXiv:1011.2268.

[76] J. Thaler and K. Van Tilburg, "Maximizing boosted top identification by minimizing N-subjettiness", *JHEP* **02** (2012) 093, doi:10.1007/JHEP02(2012)093, arXiv:1108.2701.

[77] S. D. Ellis, C. K. Vermilion, and J. R. Walsh, "Recombination algorithms and jet substructure: pruning as a tool for heavy particle searches", *Phys. Rev. D* **81** (2010) 094023, doi:10.1103/PhysRevD.81.094023, arXiv:0912.0033.

[78] CMS Collaboration, "Identification techniques for highly boosted W bosons that decay into hadrons", *JHEP* **12** (2014) 017, doi:10.1007/JHEP12(2014)017, arXiv:1410.4227.

[79] J. Gallicchio and M. D. Schwartz, "Seeing in color: jet superstructure", *Phys. Rev. Lett.* **105** (2010) 022001, doi:10.1103/PhysRevLett.105.022001, arXiv:1001.5027.

[80] E. Izaguirre, B. Shuve, and I. Yavin, "Improving identification of dijet resonances at hadron colliders", *Phys. Rev. Lett.* **114** (2015) 041802, doi:10.1103/PhysRevLett.114.041802, arXiv:1407.7037.

[81] CMS Collaboration, "V tagging observables and correlations", CMS Physics Analysis Summary CMS-PAS-JME-14-002, 2014.

[82] CMS Collaboration, "Identification of b-quark jets with the CMS experiment", *JINST* **8** (2013) P04013, doi:10.1088/1748-0221/8/04/P04013, arXiv:1211.4462.

[83] S. Ask et al., "Using γ+jets production to calibrate the Standard Model $Z(\to \nu\nu)$+jets background to new physics processes at the LHC", *JHEP* **10** (2011) 058, doi:10.1007/JHEP10(2011)058, arXiv:1107.2803.

[84] J. H. Kuhn, A. Kulesza, S. Pozzorini, and M. Schulze, "Electroweak corrections to hadronic photon production at large transverse momenta", *JHEP* **03** (2006) 059, doi:10.1088/1126-6708/2006/03/059, arXiv:hep-ph/0508253.

[85] CMS Collaboration, "Performance of b tagging at $\sqrt{s} = 8$ TeV in multijet, $\mathrm{t\bar{t}}$ and boosted topology events", CMS Physics Analysis Summary CMS-PAS-BTV-13-001, 2013.

[86] CMS Collaboration, "Measurement of the differential cross section for top quark pair production in pp collisions at $\sqrt{s} = 8$ TeV", *Eur. Phys. J. C* **75** (2015) 542, doi:10.1140/epjc/s10052-015-3709-x, arXiv:1505.04480.

[87] CMS Collaboration, "Measurement of the pp $\to$ ZZ production cross section and constraints on anomalous triple gauge couplings in four-lepton final states at $\sqrt{s} = 8$ TeV", *Phys. Lett. B* **740** (2015) 250, doi:10.1016/j.physletb.2014.11.059, arXiv:1406.0113.

[88] CMS Collaboration, "Measurement of the W^+W^- cross section in pp collisions at $\sqrt{s}$ = 8 TeV and limits on anomalous gauge couplings", (2015). arXiv:1507.03268. Submitted to *Eur. Phys. J. C*.

[89] CMS Collaboration, "CMS Luminosity Based on Pixel Cluster Counting - Summer 2013 Update", CMS Physics Analysis Summary CMS-PAS-LUM-13-001, 2013.

[90] G. Cowan, K. Cranmer, E. Gross, and O. Vitells, "Asymptotic formulae for likelihood-based tests of new physics", *Eur. Phys. J. C* **71** (2011) 1554, doi:10.1140/epjc/s10052-011-1554-0, arXiv:1007.1727. [Erratum: doi:10.1140/epjc/s10052-013-2501-z].

[91] ATLAS/CMS/LHC Higgs Combination Group Collaboration, "Procedure for the LHC Higgs boson search combination in summer 2011", Technical Report CMS-NOTE-2011-005. ATL-PHYS-PUB-2011-11, CERN, Geneva, 2011.

[92] A. L. Read, "Presentation of search results: the CL_s technique", *J. Phys. G* **28** (2002) 2693, doi:10.1088/0954-3899/28/10/313.

[93] H. An, X. Ji, and L.-T. Wang, "Light dark matter and Z' dark force at colliders", *JHEP* **07** (2012) 182, doi:10.1007/JHEP07(2012)182, arXiv:1202.2894.

[94] WMAP Collaboration, "The Microwave Anisotropy Probe (MAP) mission", *Astrophys. J.* **583** (2003) 1, doi:10.1086/345346, arXiv:astro-ph/0301158.

[95] Planck Collaboration, "The scientific programme of Planck", (2006). arXiv:astro-ph/0604069.

[96] M. Backovic et al., "Direct detection of dark matter with MadDM v.2.0", *Phys. Dark Univ.* **9-10** (2015) 37, doi:10.1016/j.dark.2015.09.001, arXiv:1505.04190.

[97] Planck Collaboration, "Planck 2013 results. XVI. Cosmological parameters", *Astron. Astrophys.* **571** (2014) A16, doi:10.1051/0004-6361/201321591, arXiv:1303.5076.

[98] T. du Pree, K. Hahn, P. Harris, and C. Roskas, "Cosmological constraints on dark matter models for collider searches", (2016). arXiv:1603.08525.

[99] S. A. Malik et al., "Interplay and characterization of dark matter searches at colliders and in direct detection experiments", *Phys. Dark Univ.* **9-10** (2015) 51, doi:10.1016/j.dark.2015.03.003, arXiv:1409.4075.

[100] P. Harris, V. V. Khoze, M. Spannowsky, and C. Williams, "Closing up on dark sectors at colliders: from 14 to 100 TeV", *Phys. Rev. D* **93** (2016) 054030, doi:10.1103/PhysRevD.93.054030, arXiv:1509.02904.

[101] G. Busoni et al., "Recommendations on presenting LHC searches for missing transverse energy signals using simplified *s*-channel models of dark matter", (2016). arXiv:1603.04156.

[102] D. S. Akerib et al., "Results from a search for dark matter in the complete LUX exposure", (2016). arXiv:1608.07648.

[103] SuperCDMS Collaboration, "New Results from the Search for Low-Mass Weakly Interacting Massive Particles with the CDMS Low Ionization Threshold Experiment", *Phys. Rev. Lett.* **116** (2016) 071301, doi:10.1103/PhysRevLett.116.071301.

[104] CRESST Collaboration, "Results on light dark matter particles with a low-threshold CRESST-II detector", *Eur. Phys. J. C* **76** (2016) 25, doi:10.1140/epjc/s10052-016-3877-3, arXiv:1509.01515.

[105] PandaX-II Collaboration, "Dark Matter Results from First 98.7-day Data of PandaX-II Experiment", *Phys. Rev. Lett.* (2016) 121303, doi:10.1103/PhysRevLett.117.121303, arXiv:1607.07400.

[106] PICO Collaboration, "Dark matter search results from the PICO-2L C_3F_8 bubble chamber", *Phys. Rev. Lett.* **114** (2015) 231302, doi:10.1103/PhysRevLett.114.231302, arXiv:1503.00008.

[107] PICO Collaboration, "Dark matter search results from the PICO-60 CF_3I bubble chamber", *Phys. Rev. D* **93** (2016) 052014, doi:10.1103/PhysRevD.93.052014, arXiv:1510.07754.

[108] IceCube Collaboration, "Improved limits on dark matter annihilation in the Sun with the 79-string IceCube detector and implications for supersymmetry", *JCAP* **04** (2016) 022, doi:10.1088/1475-7516/2016/04/022, arXiv:1601.00653.

[109] Super-Kamiokande Collaboration, "Search for neutrinos from annihilation of captured low-mass dark matter particles in the Sun by Super-Kamiokande", *Phys. Rev. Lett.* **114** (2015) 141301, doi:10.1103/PhysRevLett.114.141301, arXiv:1503.04858.

[110] Fermi-LAT Collaboration, "Constraining dark matter models from a combined analysis of milky way satellites with the Fermi large area telescope", *Phys. Rev. Lett.* **107** (2011) 241302, doi:10.1103/PhysRevLett.107.241302, arXiv:1108.3546.

[111] Fermi-LAT Collaboration, "Observations of milky way dwarf spheroidal galaxies with the Fermi-LAT detector and constraints on dark matter models", *Astrophys. J.* **712** (2010) 147, doi:10.1088/0004-637X/712/1/147, arXiv:1001.4531.

[112] O. Buchmueller, S. A. Malik, C. McCabe, and B. Penning, "Constraining dark matter interactions with pseudoscalar and scalar mediators using collider searches for multijets plus missing transverse energy", *Phys. Rev. Lett.* **115** (2015) 181802, doi:10.1103/PhysRevLett.115.181802, arXiv:1505.07826.

[113] M. R. Buckley, D. Feld, and D. Goncalves, "Scalar simplified models for dark matter", *Phys. Rev. D* **91** (2015) 015017, doi:10.1103/PhysRevD.91.015017, arXiv:1410.6497.

[114] Fermi-LAT Collaboration, "Fermi-LAT observations of high-energy γ-ray emission toward the galactic center", *Astrophys. J.* **819** (2016) 44, doi:10.3847/0004-637X/819/1/44, arXiv:1511.02938.

[115] C. Gordon and O. Macias, "Dark matter and pulsar model constraints from galactic center Fermi-LAT gamma ray observations", *Phys. Rev. D* **88** (2013) 083521, doi:10.1103/PhysRevD.88.083521, arXiv:1306.5725. [Erratum: doi:10.1103/PhysRevD.89.049901].

[116] K. N. Abazajian and M. Kaplinghat, "Detection of a gamma-ray source in the galactic center consistent with extended emission from dark matter annihilation and concentrated astrophysical emission", *Phys. Rev. D* **86** (2012) 083511, doi:10.1103/PhysRevD.86.083511, arXiv:1207.6047. [Erratum: doi:10.1103/PhysRevD.87.129902].

[117] D. Hooper and L. Goodenough, "Dark matter annihilation in the galactic center as seen by the Fermi gamma ray space telescope", *Phys. Lett. B* **697** (2011) 412, doi:10.1016/j.physletb.2011.02.029, arXiv:1010.2752.

[118] P. Agrawal, B. Batell, P. J. Fox, and R. Harnik, "WIMPs at the galactic center", *JCAP* **05** (2015) 011, doi:10.1088/1475-7516/2015/05/011, arXiv:1411.2592.

[119] F. Calore, I. Cholis, C. McCabe, and C. Weniger, "A tale of tails: dark matter interpretations of the Fermi GeV excess in light of background model systematics", *Phys. Rev. D* **91** (2015) 063003, doi:10.1103/PhysRevD.91.063003, arXiv:1411.4647.

A Supplementary Material

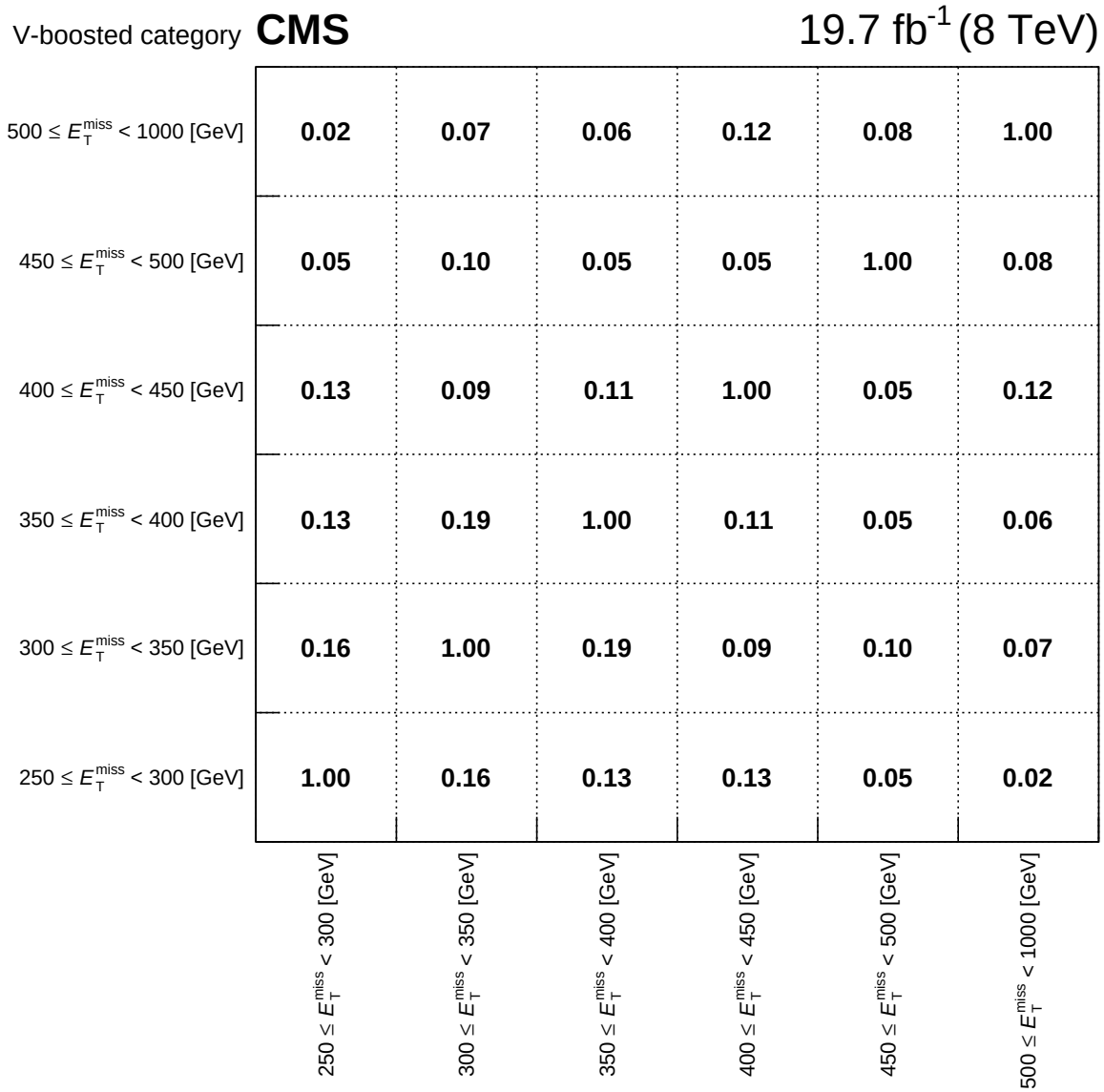

Figure 12: Correlations between the predicted number of background events in each bin of $E_{\mathrm{T}}^{\mathrm{miss}}$ in the V-boosted category. The correlation is determined from the simultaneous fit to data in the dimuon, single muon, and photon control regions in all the three event categories.

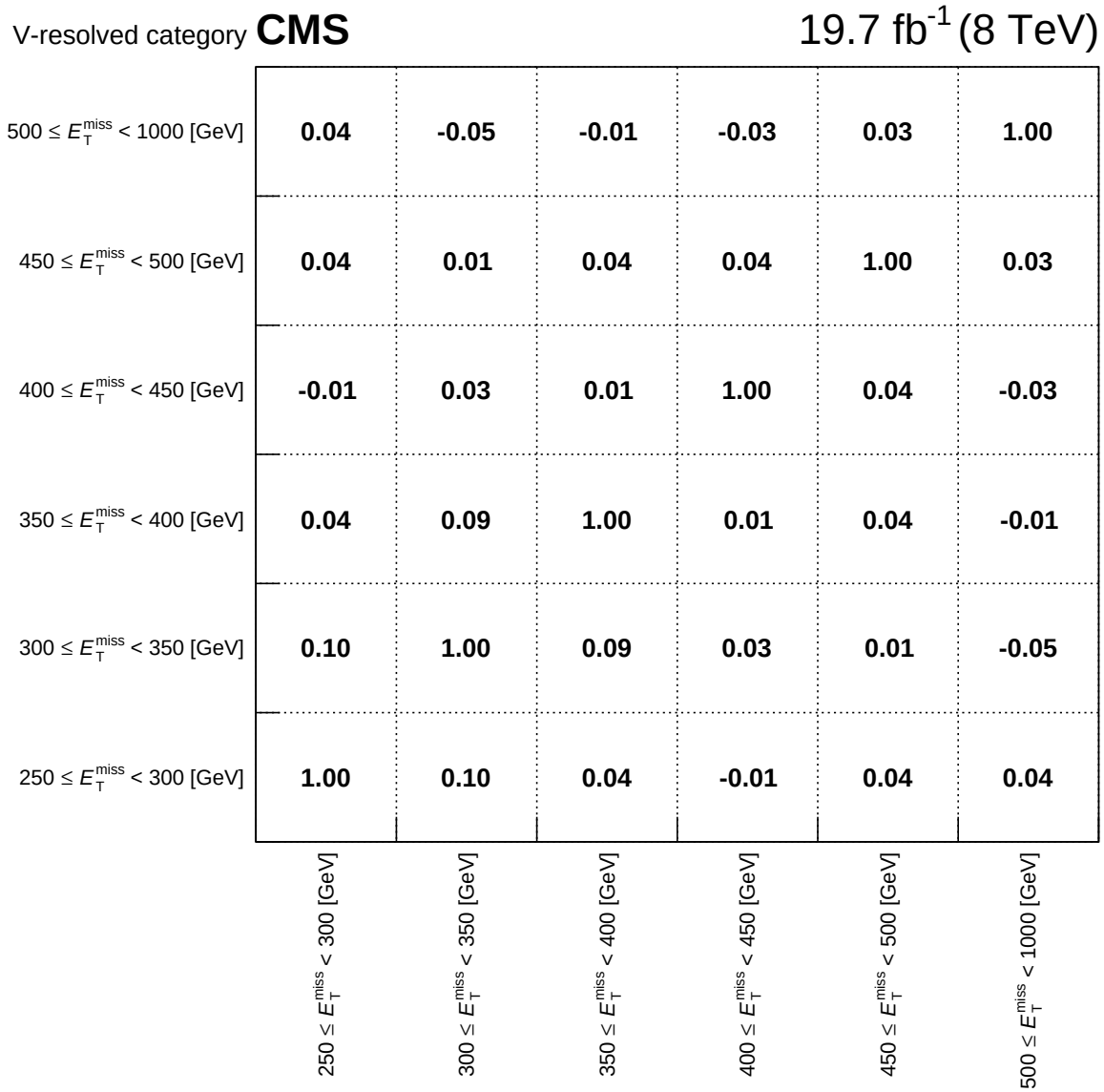

Figure 13: Correlations between the predicted number of background events in each bin of $E_{\mathrm{T}}^{\mathrm{miss}}$ in the V-resolved category. The correlation is determined from the simultaneous fit to data in the dimuon, single muon, and photon control regions in all the three event categories.

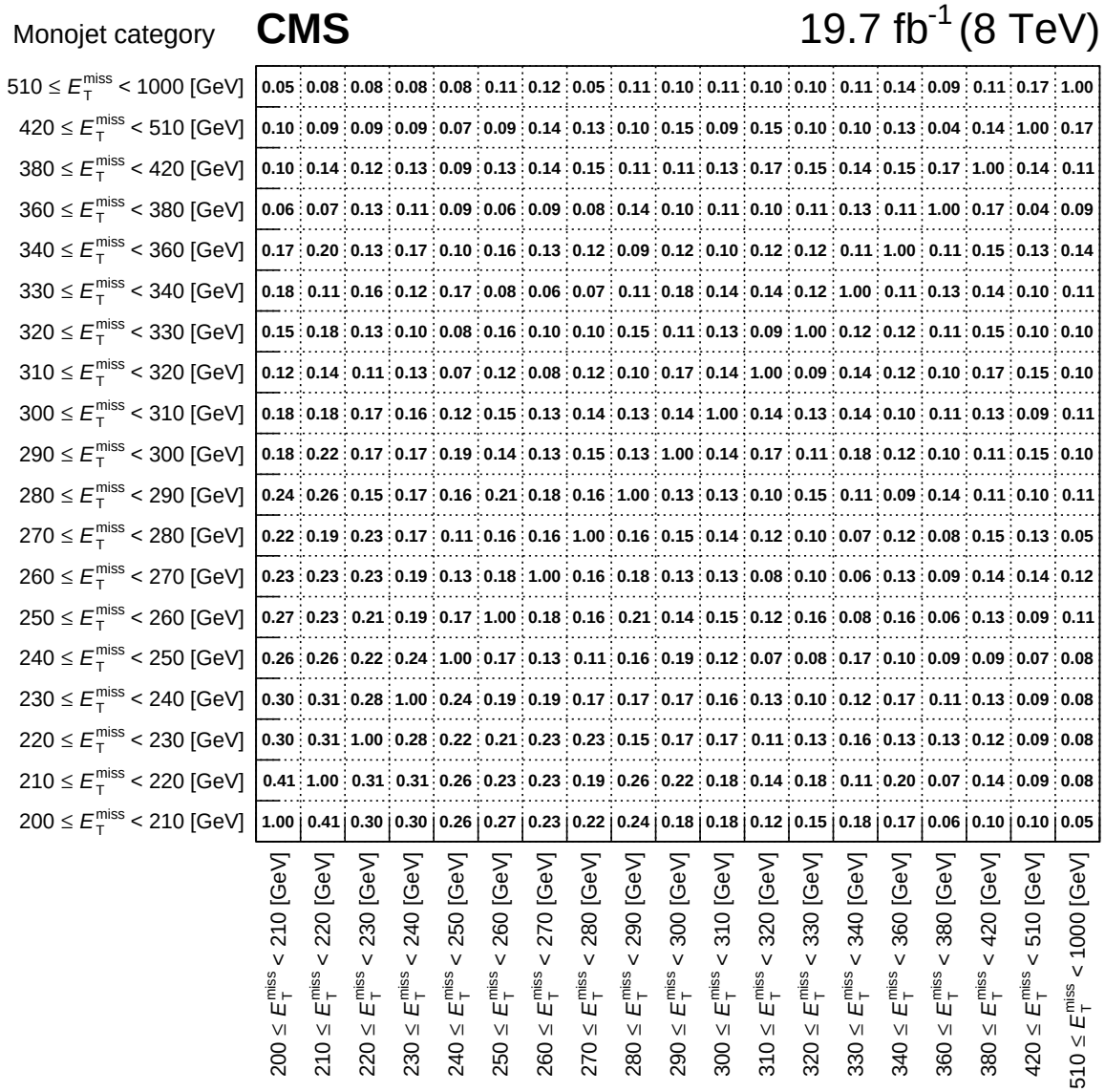

Figure 14: Correlations between the predicted number of background events in each bin of $E_{\mathrm{T}}^{\mathrm{miss}}$ in the monojet category. The correlation is determined from the simultaneous fit to data in the dimuon, single muon, and photon control regions in all the three event categories.

B The CMS Collaboration

Yerevan Physics Institute, Yerevan, Armenia
V. Khachatryan, A.M. Sirunyan, A. Tumasyan

Institut für Hochenergiephysik der OeAW, Wien, Austria
W. Adam, E. Asilar, T. Bergauer, J. Brandstetter, E. Brondolin, M. Dragicevic, J. Erö, M. Flechl, M. Friedl, R. Frühwirth[1], V.M. Ghete, C. Hartl, N. Hörmann, J. Hrubec, M. Jeitler[1], A. König, I. Krätschmer, D. Liko, T. Matsushita, I. Mikulec, D. Rabady, N. Rad, B. Rahbaran, H. Rohringer, J. Schieck[1], J. Strauss, W. Treberer-Treberspurg, W. Waltenberger, C.-E. Wulz[1]

National Centre for Particle and High Energy Physics, Minsk, Belarus
V. Mossolov, N. Shumeiko, J. Suarez Gonzalez

Universiteit Antwerpen, Antwerpen, Belgium
S. Alderweireldt, E.A. De Wolf, X. Janssen, J. Lauwers, M. Van De Klundert, H. Van Haevermaet, P. Van Mechelen, N. Van Remortel, A. Van Spilbeeck

Vrije Universiteit Brussel, Brussel, Belgium
S. Abu Zeid, F. Blekman, J. D'Hondt, N. Daci, I. De Bruyn, K. Deroover, N. Heracleous, S. Lowette, S. Moortgat, L. Moreels, A. Olbrechts, Q. Python, S. Tavernier, W. Van Doninck, P. Van Mulders, I. Van Parijs

Université Libre de Bruxelles, Bruxelles, Belgium
H. Brun, C. Caillol, B. Clerbaux, G. De Lentdecker, H. Delannoy, G. Fasanella, L. Favart, R. Goldouzian, A. Grebenyuk, G. Karapostoli, T. Lenzi, A. Léonard, J. Luetic, T. Maerschalk, A. Marinov, A. Randle-conde, T. Seva, C. Vander Velde, P. Vanlaer, R. Yonamine, F. Zenoni, F. Zhang[2]

Ghent University, Ghent, Belgium
A. Cimmino, T. Cornelis, D. Dobur, A. Fagot, G. Garcia, M. Gul, D. Poyraz, S. Salva, R. Schöfbeck, M. Tytgat, W. Van Driessche, E. Yazgan, N. Zaganidis

Université Catholique de Louvain, Louvain-la-Neuve, Belgium
H. Bakhshiansohi, C. Beluffi[3], O. Bondu, S. Brochet, G. Bruno, A. Caudron, S. De Visscher, C. Delaere, M. Delcourt, L. Forthomme, B. Francois, A. Giammanco, A. Jafari, P. Jez, M. Komm, V. Lemaitre, A. Magitteri, A. Mertens, M. Musich, C. Nuttens, K. Piotrzkowski, L. Quertenmont, M. Selvaggi, M. Vidal Marono, S. Wertz

Université de Mons, Mons, Belgium
N. Beliy

Centro Brasileiro de Pesquisas Fisicas, Rio de Janeiro, Brazil
W.L. Aldá Júnior, F.L. Alves, G.A. Alves, L. Brito, C. Hensel, A. Moraes, M.E. Pol, P. Rebello Teles

Universidade do Estado do Rio de Janeiro, Rio de Janeiro, Brazil
E. Belchior Batista Das Chagas, W. Carvalho, J. Chinellato[4], A. Custódio, E.M. Da Costa, G.G. Da Silveira, D. De Jesus Damiao, C. De Oliveira Martins, S. Fonseca De Souza, L.M. Huertas Guativa, H. Malbouisson, D. Matos Figueiredo, C. Mora Herrera, L. Mundim, H. Nogima, W.L. Prado Da Silva, A. Santoro, A. Sznajder, E.J. Tonelli Manganote[4], A. Vilela Pereira

Universidade Estadual Paulista [a], Universidade Federal do ABC [b], São Paulo, Brazil
S. Ahuja[a], C.A. Bernardes[b], S. Dogra[a], T.R. Fernandez Perez Tomei[a], E.M. Gregores[b],

P.G. Mercadante[b], C.S. Moon[a], S.F. Novaes[a], Sandra S. Padula[a], D. Romero Abad[b], J.C. Ruiz Vargas

Institute for Nuclear Research and Nuclear Energy, Sofia, Bulgaria
A. Aleksandrov, R. Hadjiiska, P. Iaydjiev, M. Rodozov, S. Stoykova, G. Sultanov, M. Vutova

University of Sofia, Sofia, Bulgaria
A. Dimitrov, I. Glushkov, L. Litov, B. Pavlov, P. Petkov

Beihang University, Beijing, China
W. Fang[5]

Institute of High Energy Physics, Beijing, China
M. Ahmad, J.G. Bian, G.M. Chen, H.S. Chen, M. Chen, Y. Chen[6], T. Cheng, C.H. Jiang, D. Leggat, Z. Liu, F. Romeo, S.M. Shaheen, A. Spiezia, J. Tao, C. Wang, Z. Wang, H. Zhang, J. Zhao

State Key Laboratory of Nuclear Physics and Technology, Peking University, Beijing, China
Y. Ban, G. Chen, Q. Li, S. Liu, Y. Mao, S.J. Qian, D. Wang, Z. Xu

Universidad de Los Andes, Bogota, Colombia
C. Avila, A. Cabrera, L.F. Chaparro Sierra, C. Florez, J.P. Gomez, C.F. González Hernández, J.D. Ruiz Alvarez, J.C. Sanabria

University of Split, Faculty of Electrical Engineering, Mechanical Engineering and Naval Architecture, Split, Croatia
N. Godinovic, D. Lelas, I. Puljak, P.M. Ribeiro Cipriano

University of Split, Faculty of Science, Split, Croatia
Z. Antunovic, M. Kovac

Institute Rudjer Boskovic, Zagreb, Croatia
V. Brigljevic, D. Ferencek, K. Kadija, S. Micanovic, L. Sudic, T. Susa

University of Cyprus, Nicosia, Cyprus
A. Attikis, G. Mavromanolakis, J. Mousa, C. Nicolaou, F. Ptochos, P.A. Razis, H. Rykaczewski

Charles University, Prague, Czech Republic
M. Finger[7], M. Finger Jr.[7]

Universidad San Francisco de Quito, Quito, Ecuador
E. Carrera Jarrin

Academy of Scientific Research and Technology of the Arab Republic of Egypt, Egyptian Network of High Energy Physics, Cairo, Egypt
A.A. Abdelalim[8,9], Y. Mohammed[10], E. Salama[11,12]

National Institute of Chemical Physics and Biophysics, Tallinn, Estonia
B. Calpas, M. Kadastik, M. Murumaa, L. Perrini, M. Raidal, A. Tiko, C. Veelken

Department of Physics, University of Helsinki, Helsinki, Finland
P. Eerola, J. Pekkanen, M. Voutilainen

Helsinki Institute of Physics, Helsinki, Finland
J. Härkönen, V. Karimäki, R. Kinnunen, T. Lampén, K. Lassila-Perini, S. Lehti, T. Lindén, P. Luukka, T. Peltola, J. Tuominiemi, E. Tuovinen, L. Wendland

Lappeenranta University of Technology, Lappeenranta, Finland
J. Talvitie, T. Tuuva

IRFU, CEA, Université Paris-Saclay, Gif-sur-Yvette, France
M. Besancon, F. Couderc, M. Dejardin, D. Denegri, B. Fabbro, J.L. Faure, C. Favaro, F. Ferri, S. Ganjour, S. Ghosh, A. Givernaud, P. Gras, G. Hamel de Monchenault, P. Jarry, I. Kucher, E. Locci, M. Machet, J. Malcles, J. Rander, A. Rosowsky, M. Titov, A. Zghiche

Laboratoire Leprince-Ringuet, Ecole Polytechnique, IN2P3-CNRS, Palaiseau, France
A. Abdulsalam, I. Antropov, S. Baffioni, F. Beaudette, P. Busson, L. Cadamuro, E. Chapon, C. Charlot, O. Davignon, R. Granier de Cassagnac, M. Jo, S. Lisniak, P. Miné, M. Nguyen, C. Ochando, G. Ortona, P. Paganini, P. Pigard, S. Regnard, R. Salerno, Y. Sirois, T. Strebler, Y. Yilmaz, A. Zabi

Institut Pluridisciplinaire Hubert Curien, Université de Strasbourg, Université de Haute Alsace Mulhouse, CNRS/IN2P3, Strasbourg, France
J.-L. Agram[13], J. Andrea, A. Aubin, D. Bloch, J.-M. Brom, M. Buttignol, E.C. Chabert, N. Chanon, C. Collard, E. Conte[13], X. Coubez, J.-C. Fontaine[13], D. Gelé, U. Goerlach, A.-C. Le Bihan, J.A. Merlin[14], K. Skovpen, P. Van Hove

Centre de Calcul de l'Institut National de Physique Nucleaire et de Physique des Particules, CNRS/IN2P3, Villeurbanne, France
S. Gadrat

Université de Lyon, Université Claude Bernard Lyon 1, CNRS-IN2P3, Institut de Physique Nucléaire de Lyon, Villeurbanne, France
S. Beauceron, C. Bernet, G. Boudoul, E. Bouvier, C.A. Carrillo Montoya, R. Chierici, D. Contardo, B. Courbon, P. Depasse, H. El Mamouni, J. Fan, J. Fay, S. Gascon, M. Gouzevitch, G. Grenier, B. Ille, F. Lagarde, I.B. Laktineh, M. Lethuillier, L. Mirabito, A.L. Pequegnot, S. Perries, A. Popov[15], D. Sabes, V. Sordini, M. Vander Donckt, P. Verdier, S. Viret

Georgian Technical University, Tbilisi, Georgia
T. Toriashvili[16]

Tbilisi State University, Tbilisi, Georgia
Z. Tsamalaidze[7]

RWTH Aachen University, I. Physikalisches Institut, Aachen, Germany
C. Autermann, S. Beranek, L. Feld, A. Heister, M.K. Kiesel, K. Klein, M. Lipinski, A. Ostapchuk, M. Preuten, F. Raupach, S. Schael, C. Schomakers, J.F. Schulte, J. Schulz, T. Verlage, H. Weber, V. Zhukov[15]

RWTH Aachen University, III. Physikalisches Institut A, Aachen, Germany
M. Brodski, E. Dietz-Laursonn, D. Duchardt, M. Endres, M. Erdmann, S. Erdweg, T. Esch, R. Fischer, A. Güth, M. Hamer, T. Hebbeker, C. Heidemann, K. Hoepfner, S. Knutzen, M. Merschmeyer, A. Meyer, P. Millet, S. Mukherjee, M. Olschewski, K. Padeken, T. Pook, M. Radziej, H. Reithler, M. Rieger, F. Scheuch, L. Sonnenschein, D. Teyssier, S. Thüer

RWTH Aachen University, III. Physikalisches Institut B, Aachen, Germany
V. Cherepanov, G. Flügge, W. Haj Ahmad, F. Hoehle, B. Kargoll, T. Kress, A. Künsken, J. Lingemann, A. Nehrkorn, A. Nowack, I.M. Nugent, C. Pistone, O. Pooth, A. Stahl[14]

Deutsches Elektronen-Synchrotron, Hamburg, Germany
M. Aldaya Martin, C. Asawatangtrakuldee, K. Beernaert, O. Behnke, U. Behrens, A.A. Bin Anuar, K. Borras[17], A. Campbell, P. Connor, C. Contreras-Campana, F. Costanza, C. Diez

Pardos, G. Dolinska, G. Eckerlin, D. Eckstein, E. Eren, E. Gallo[18], J. Garay Garcia, A. Geiser, A. Gizhko, J.M. Grados Luyando, P. Gunnellini, A. Harb, J. Hauk, M. Hempel[19], H. Jung, A. Kalogeropoulos, O. Karacheban[19], M. Kasemann, J. Keaveney, J. Kieseler, C. Kleinwort, I. Korol, D. Krücker, W. Lange, A. Lelek, J. Leonard, K. Lipka, A. Lobanov, W. Lohmann[19], R. Mankel, I.-A. Melzer-Pellmann, A.B. Meyer, G. Mittag, J. Mnich, A. Mussgiller, E. Ntomari, D. Pitzl, R. Placakyte, A. Raspereza, B. Roland, M.Ö. Sahin, P. Saxena, T. Schoerner-Sadenius, C. Seitz, S. Spannagel, N. Stefaniuk, K.D. Trippkewitz, G.P. Van Onsem, R. Walsh, C. Wissing

University of Hamburg, Hamburg, Germany
V. Blobel, M. Centis Vignali, A.R. Draeger, T. Dreyer, E. Garutti, K. Goebel, D. Gonzalez, J. Haller, M. Hoffmann, A. Junkes, R. Klanner, R. Kogler, N. Kovalchuk, T. Lapsien, T. Lenz, I. Marchesini, D. Marconi, M. Meyer, M. Niedziela, D. Nowatschin, J. Ott, F. Pantaleo[14], T. Peiffer, A. Perieanu, J. Poehlsen, C. Sander, C. Scharf, P. Schleper, A. Schmidt, S. Schumann, J. Schwandt, H. Stadie, G. Steinbrück, F.M. Stober, M. Stöver, H. Tholen, D. Troendle, E. Usai, L. Vanelderen, A. Vanhoefer, B. Vormwald

Institut für Experimentelle Kernphysik, Karlsruhe, Germany
C. Barth, C. Baus, J. Berger, E. Butz, T. Chwalek, F. Colombo, W. De Boer, A. Dierlamm, S. Fink, R. Friese, M. Giffels, A. Gilbert, P. Goldenzweig, D. Haitz, F. Hartmann[14], S.M. Heindl, U. Husemann, I. Katkov[15], P. Lobelle Pardo, B. Maier, H. Mildner, M.U. Mozer, T. Müller, Th. Müller, M. Plagge, G. Quast, K. Rabbertz, S. Röcker, F. Roscher, M. Schröder, I. Shvetsov, G. Sieber, H.J. Simonis, R. Ulrich, J. Wagner-Kuhr, S. Wayand, M. Weber, T. Weiler, S. Williamson, C. Wöhrmann, R. Wolf

Institute of Nuclear and Particle Physics (INPP), NCSR Demokritos, Aghia Paraskevi, Greece
G. Anagnostou, G. Daskalakis, T. Geralis, V.A. Giakoumopoulou, A. Kyriakis, D. Loukas, I. Topsis-Giotis

National and Kapodistrian University of Athens, Athens, Greece
A. Agapitos, S. Kesisoglou, A. Panagiotou, N. Saoulidou, E. Tziaferi

University of Ioánnina, Ioánnina, Greece
I. Evangelou, G. Flouris, C. Foudas, P. Kokkas, N. Loukas, N. Manthos, I. Papadopoulos, E. Paradas

MTA-ELTE Lendület CMS Particle and Nuclear Physics Group, Eötvös Loránd University, Budapest, Hungary
N. Filipovic

Wigner Research Centre for Physics, Budapest, Hungary
G. Bencze, C. Hajdu, P. Hidas, D. Horvath[20], F. Sikler, V. Veszpremi, G. Vesztergombi[21], A.J. Zsigmond

Institute of Nuclear Research ATOMKI, Debrecen, Hungary
N. Beni, S. Czellar, J. Karancsi[22], A. Makovec, J. Molnar, Z. Szillasi

University of Debrecen, Debrecen, Hungary
M. Bartók[21], P. Raics, Z.L. Trocsanyi, B. Ujvari

National Institute of Science Education and Research, Bhubaneswar, India
S. Bahinipati, S. Choudhury[23], P. Mal, K. Mandal, A. Nayak[24], D.K. Sahoo, N. Sahoo, S.K. Swain

Panjab University, Chandigarh, India
S. Bansal, S.B. Beri, V. Bhatnagar, R. Chawla, U.Bhawandeep, A.K. Kalsi, A. Kaur, M. Kaur, R. Kumar, A. Mehta, M. Mittal, J.B. Singh, G. Walia

University of Delhi, Delhi, India
Ashok Kumar, A. Bhardwaj, B.C. Choudhary, R.B. Garg, S. Keshri, S. Malhotra, M. Naimuddin, N. Nishu, K. Ranjan, R. Sharma, V. Sharma

Saha Institute of Nuclear Physics, Kolkata, India
R. Bhattacharya, S. Bhattacharya, K. Chatterjee, S. Dey, S. Dutt, S. Dutta, S. Ghosh, N. Majumdar, A. Modak, K. Mondal, S. Mukhopadhyay, S. Nandan, A. Purohit, A. Roy, D. Roy, S. Roy Chowdhury, S. Sarkar, M. Sharan, S. Thakur

Indian Institute of Technology Madras, Madras, India
P.K. Behera

Bhabha Atomic Research Centre, Mumbai, India
R. Chudasama, D. Dutta, V. Jha, V. Kumar, A.K. Mohanty[14], P.K. Netrakanti, L.M. Pant, P. Shukla, A. Topkar

Tata Institute of Fundamental Research-A, Mumbai, India
T. Aziz, S. Dugad, G. Kole, B. Mahakud, S. Mitra, G.B. Mohanty, B. Parida, N. Sur, B. Sutar

Tata Institute of Fundamental Research-B, Mumbai, India
S. Banerjee, S. Bhowmik[25], R.K. Dewanjee, S. Ganguly, M. Guchait, Sa. Jain, S. Kumar, M. Maity[25], G. Majumder, K. Mazumdar, T. Sarkar[25], N. Wickramage[26]

Indian Institute of Science Education and Research (IISER), Pune, India
S. Chauhan, S. Dube, V. Hegde, A. Kapoor, K. Kothekar, A. Rane, S. Sharma

Institute for Research in Fundamental Sciences (IPM), Tehran, Iran
H. Behnamian, S. Chenarani[27], E. Eskandari Tadavani, S.M. Etesami[27], A. Fahim[28], M. Khakzad, M. Mohammadi Najafabadi, M. Naseri, S. Paktinat Mehdiabadi, F. Rezaei Hosseinabadi, B. Safarzadeh[29], M. Zeinali

University College Dublin, Dublin, Ireland
M. Felcini, M. Grunewald

INFN Sezione di Bari [a], Università di Bari [b], Politecnico di Bari [c], Bari, Italy
M. Abbrescia[a,b], C. Calabria[a,b], C. Caputo[a,b], A. Colaleo[a], D. Creanza[a,c], L. Cristella[a,b], N. De Filippis[a,c], M. De Palma[a,b], L. Fiore[a], G. Iaselli[a,c], G. Maggi[a,c], M. Maggi[a], G. Miniello[a,b], S. My[a,b], S. Nuzzo[a,b], A. Pompili[a,b], G. Pugliese[a,c], R. Radogna[a,b], A. Ranieri[a], G. Selvaggi[a,b], L. Silvestris[a,14], R. Venditti[a,b], P. Verwilligen[a]

INFN Sezione di Bologna [a], Università di Bologna [b], Bologna, Italy
G. Abbiendi[a], C. Battilana, D. Bonacorsi[a,b], S. Braibant-Giacomelli[a,b], L. Brigliadori[a,b], R. Campanini[a,b], P. Capiluppi[a,b], A. Castro[a,b], F.R. Cavallo[a], S.S. Chhibra[a,b], G. Codispoti[a,b], M. Cuffiani[a,b], G.M. Dallavalle[a], F. Fabbri[a], A. Fanfani[a,b], D. Fasanella[a,b], P. Giacomelli[a], C. Grandi[a], L. Guiducci[a,b], S. Marcellini[a], G. Masetti[a], A. Montanari[a], F.L. Navarria[a,b], A. Perrotta[a], A.M. Rossi[a,b], T. Rovelli[a,b], G.P. Siroli[a,b], N. Tosi[a,b,14]

INFN Sezione di Catania [a], Università di Catania [b], Catania, Italy
S. Albergo[a,b], M. Chiorboli[a,b], S. Costa[a,b], A. Di Mattia[a], F. Giordano[a,b], R. Potenza[a,b], A. Tricomi[a,b], C. Tuve[a,b]

INFN Sezione di Firenze [a], Università di Firenze [b], Firenze, Italy
G. Barbagli[a], V. Ciulli[a,b], C. Civinini[a], R. D'Alessandro[a,b], E. Focardi[a,b], V. Gori[a,b], P. Lenzi[a,b], M. Meschini[a], S. Paoletti[a], G. Sguazzoni[a], L. Viliani[a,b,14]

INFN Laboratori Nazionali di Frascati, Frascati, Italy
L. Benussi, S. Bianco, F. Fabbri, D. Piccolo, F. Primavera[14]

INFN Sezione di Genova [a], Università di Genova [b], Genova, Italy
V. Calvelli[a,b], F. Ferro[a], M. Lo Vetere[a,b], M.R. Monge[a,b], E. Robutti[a], S. Tosi[a,b]

INFN Sezione di Milano-Bicocca [a], Università di Milano-Bicocca [b], Milano, Italy
L. Brianza[14], M.E. Dinardo[a,b], S. Fiorendi[a,b], S. Gennai[a], A. Ghezzi[a,b], P. Govoni[a,b], S. Malvezzi[a], R.A. Manzoni[a,b,14], B. Marzocchi[a,b], D. Menasce[a], L. Moroni[a], M. Paganoni[a,b], D. Pedrini[a], S. Pigazzini, S. Ragazzi[a,b], T. Tabarelli de Fatis[a,b]

INFN Sezione di Napoli [a], Università di Napoli 'Federico II' [b], Napoli, Italy, Università della Basilicata [c], Potenza, Italy, Università G. Marconi [d], Roma, Italy
S. Buontempo[a], N. Cavallo[a,c], G. De Nardo, S. Di Guida[a,d,14], M. Esposito[a,b], F. Fabozzi[a,c], A.O.M. Iorio[a,b], G. Lanza[a], L. Lista[a], S. Meola[a,d,14], P. Paolucci[a,14], C. Sciacca[a,b], F. Thyssen

INFN Sezione di Padova [a], Università di Padova [b], Padova, Italy, Università di Trento [c], Trento, Italy
P. Azzi[a,14], N. Bacchetta[a], L. Benato[a,b], D. Bisello[a,b], A. Boletti[a,b], R. Carlin[a,b], A. Carvalho Antunes De Oliveira[a,b], P. Checchia[a], M. Dall'Osso[a,b], P. De Castro Manzano[a], T. Dorigo[a], U. Dosselli[a], F. Gasparini[a,b], U. Gasparini[a,b], A. Gozzelino[a], S. Lacaprara[a], M. Margoni[a,b], A.T. Meneguzzo[a,b], J. Pazzini[a,b,14], N. Pozzobon[a,b], P. Ronchese[a,b], F. Simonetto[a,b], E. Torassa[a], M. Zanetti, P. Zotto[a,b], A. Zucchetta[a,b], G. Zumerle[a,b]

INFN Sezione di Pavia [a], Università di Pavia [b], Pavia, Italy
A. Braghieri[a], A. Magnani[a,b], P. Montagna[a,b], S.P. Ratti[a,b], V. Re[a], C. Riccardi[a,b], P. Salvini[a], I. Vai[a,b], P. Vitulo[a,b]

INFN Sezione di Perugia [a], Università di Perugia [b], Perugia, Italy
L. Alunni Solestizi[a,b], G.M. Bilei[a], D. Ciangottini[a,b], L. Fanò[a,b], P. Lariccia[a,b], R. Leonardi[a,b], G. Mantovani[a,b], M. Menichelli[a], A. Saha[a], A. Santocchia[a,b]

INFN Sezione di Pisa [a], Università di Pisa [b], Scuola Normale Superiore di Pisa [c], Pisa, Italy
K. Androsov[a,30], P. Azzurri[a,14], G. Bagliesi[a], J. Bernardini[a], T. Boccali[a], R. Castaldi[a], M.A. Ciocci[a,30], R. Dell'Orso[a], S. Donato[a,c], G. Fedi, A. Giassi[a], M.T. Grippo[a,30], F. Ligabue[a,c], T. Lomtadze[a], L. Martini[a,b], A. Messineo[a,b], F. Palla[a], A. Rizzi[a,b], A. Savoy-Navarro[a,31], P. Spagnolo[a], R. Tenchini[a], G. Tonelli[a,b], A. Venturi[a], P.G. Verdini[a]

INFN Sezione di Roma [a], Università di Roma [b], Roma, Italy
L. Barone[a,b], F. Cavallari[a], M. Cipriani[a,b], G. D'imperio[a,b,14], D. Del Re[a,b,14], M. Diemoz[a], S. Gelli[a,b], C. Jorda[a], E. Longo[a,b], F. Margaroli[a,b], P. Meridiani[a], G. Organtini[a,b], R. Paramatti[a], F. Preiato[a,b], S. Rahatlou[a,b], C. Rovelli[a], F. Santanastasio[a,b]

INFN Sezione di Torino [a], Università di Torino [b], Torino, Italy, Università del Piemonte Orientale [c], Novara, Italy
N. Amapane[a,b], R. Arcidiacono[a,c,14], S. Argiro[a,b], M. Arneodo[a,c], N. Bartosik[a], R. Bellan[a,b], C. Biino[a], N. Cartiglia[a], F. Cenna[a,b], M. Costa[a,b], R. Covarelli[a,b], A. Degano[a,b], N. Demaria[a], L. Finco[a,b], B. Kiani[a,b], C. Mariotti[a], S. Maselli[a], E. Migliore[a,b], V. Monaco[a,b], E. Monteil[a,b], M.M. Obertino[a,b], L. Pacher[a,b], N. Pastrone[a], M. Pelliccioni[a], G.L. Pinna Angioni[a,b], F. Ravera[a,b],

A. Romero[a,b], M. Ruspa[a,c], R. Sacchi[a,b], K. Shchelina[a,b], V. Sola[a], A. Solano[a,b], A. Staiano[a], P. Traczyk[a,b]

INFN Sezione di Trieste [a], Università di Trieste [b], Trieste, Italy
S. Belforte[a], M. Casarsa[a], F. Cossutti[a], G. Della Ricca[a,b], C. La Licata[a,b], A. Schizzi[a,b], A. Zanetti[a]

Kyungpook National University, Daegu, Korea
D.H. Kim, G.N. Kim, M.S. Kim, S. Lee, S.W. Lee, Y.D. Oh, S. Sekmen, D.C. Son, Y.C. Yang

Chonbuk National University, Jeonju, Korea
A. Lee

Hanyang University, Seoul, Korea
J.A. Brochero Cifuentes, T.J. Kim

Korea University, Seoul, Korea
S. Cho, S. Choi, Y. Go, D. Gyun, S. Ha, B. Hong, Y. Jo, Y. Kim, B. Lee, K. Lee, K.S. Lee, S. Lee, J. Lim, S.K. Park, Y. Roh

Seoul National University, Seoul, Korea
J. Almond, J. Kim, S.B. Oh, S.h. Seo, U.K. Yang, H.D. Yoo, G.B. Yu

University of Seoul, Seoul, Korea
M. Choi, H. Kim, H. Kim, J.H. Kim, J.S.H. Lee, I.C. Park, G. Ryu, M.S. Ryu

Sungkyunkwan University, Suwon, Korea
Y. Choi, J. Goh, C. Hwang, J. Lee, I. Yu

Vilnius University, Vilnius, Lithuania
V. Dudenas, A. Juodagalvis, J. Vaitkus

National Centre for Particle Physics, Universiti Malaya, Kuala Lumpur, Malaysia
I. Ahmed, Z.A. Ibrahim, J.R. Komaragiri, M.A.B. Md Ali[32], F. Mohamad Idris[33], W.A.T. Wan Abdullah, M.N. Yusli, Z. Zolkapli

Centro de Investigacion y de Estudios Avanzados del IPN, Mexico City, Mexico
H. Castilla-Valdez, E. De La Cruz-Burelo, I. Heredia-De La Cruz[34], A. Hernandez-Almada, R. Lopez-Fernandez, R. Magaña Villalba, J. Mejia Guisao, A. Sanchez-Hernandez

Universidad Iberoamericana, Mexico City, Mexico
S. Carrillo Moreno, C. Oropeza Barrera, F. Vazquez Valencia

Benemerita Universidad Autonoma de Puebla, Puebla, Mexico
S. Carpinteyro, I. Pedraza, H.A. Salazar Ibarguen, C. Uribe Estrada

Universidad Autónoma de San Luis Potosí, San Luis Potosí, Mexico
A. Morelos Pineda

University of Auckland, Auckland, New Zealand
D. Krofcheck

University of Canterbury, Christchurch, New Zealand
P.H. Butler

National Centre for Physics, Quaid-I-Azam University, Islamabad, Pakistan
A. Ahmad, M. Ahmad, Q. Hassan, H.R. Hoorani, W.A. Khan, M.A. Shah, M. Shoaib, M. Waqas

National Centre for Nuclear Research, Swierk, Poland
H. Bialkowska, M. Bluj, B. Boimska, T. Frueboes, M. Górski, M. Kazana, K. Nawrocki, K. Romanowska-Rybinska, M. Szleper, P. Zalewski

Institute of Experimental Physics, Faculty of Physics, University of Warsaw, Warsaw, Poland
K. Bunkowski, A. Byszuk[35], K. Doroba, A. Kalinowski, M. Konecki, J. Krolikowski, M. Misiura, M. Olszewski, M. Walczak

Laboratório de Instrumentação e Física Experimental de Partículas, Lisboa, Portugal
P. Bargassa, C. Beirão Da Cruz E Silva, A. Di Francesco, P. Faccioli, P.G. Ferreira Parracho, M. Gallinaro, J. Hollar, N. Leonardo, L. Lloret Iglesias, M.V. Nemallapudi, J. Rodrigues Antunes, J. Seixas, O. Toldaiev, D. Vadruccio, J. Varela, P. Vischia

Joint Institute for Nuclear Research, Dubna, Russia
S. Afanasiev, P. Bunin, M. Gavrilenko, I. Golutvin, I. Gorbunov, A. Kamenev, V. Karjavin, A. Lanev, A. Malakhov, V. Matveev[36,37], P. Moisenz, V. Palichik, V. Perelygin, S. Shmatov, S. Shulha, N. Skatchkov, V. Smirnov, N. Voytishin, A. Zarubin

Petersburg Nuclear Physics Institute, Gatchina (St. Petersburg), Russia
L. Chtchipounov, V. Golovtsov, Y. Ivanov, V. Kim[38], E. Kuznetsova[39], V. Murzin, V. Oreshkin, V. Sulimov, A. Vorobyev

Institute for Nuclear Research, Moscow, Russia
Yu. Andreev, A. Dermenev, S. Gninenko, N. Golubev, A. Karneyeu, M. Kirsanov, N. Krasnikov, A. Pashenkov, D. Tlisov, A. Toropin

Institute for Theoretical and Experimental Physics, Moscow, Russia
V. Epshteyn, V. Gavrilov, N. Lychkovskaya, V. Popov, I. Pozdnyakov, G. Safronov, A. Spiridonov, M. Toms, E. Vlasov, A. Zhokin

MIPT
A. Bylinkin[37]

National Research Nuclear University 'Moscow Engineering Physics Institute' (MEPhI), Moscow, Russia
R. Chistov[40], M. Danilov[40], V. Rusinov

P.N. Lebedev Physical Institute, Moscow, Russia
V. Andreev, M. Azarkin[37], I. Dremin[37], M. Kirakosyan, A. Leonidov[37], S.V. Rusakov, A. Terkulov

Skobeltsyn Institute of Nuclear Physics, Lomonosov Moscow State University, Moscow, Russia
A. Baskakov, A. Belyaev, E. Boos, M. Dubinin[41], L. Dudko, A. Ershov, A. Gribushin, V. Klyukhin, O. Kodolova, I. Lokhtin, I. Miagkov, S. Obraztsov, S. Petrushanko, V. Savrin, A. Snigirev

Novosibirsk State University (NSU), Novosibirsk, Russia
V. Blinov[42], Y.Skovpen[42]

State Research Center of Russian Federation, Institute for High Energy Physics, Protvino, Russia
I. Azhgirey, I. Bayshev, S. Bitioukov, D. Elumakhov, V. Kachanov, A. Kalinin, D. Konstantinov, V. Krychkine, V. Petrov, R. Ryutin, A. Sobol, S. Troshin, N. Tyurin, A. Uzunian, A. Volkov

University of Belgrade, Faculty of Physics and Vinca Institute of Nuclear Sciences, Belgrade, Serbia
P. Adzic[43], P. Cirkovic, D. Devetak, M. Dordevic, J. Milosevic, V. Rekovic

Centro de Investigaciones Energéticas Medioambientales y Tecnológicas (CIEMAT), Madrid, Spain
J. Alcaraz Maestre, M. Barrio Luna, E. Calvo, M. Cerrada, M. Chamizo Llatas, N. Colino, B. De La Cruz, A. Delgado Peris, A. Escalante Del Valle, C. Fernandez Bedoya, J.P. Fernández Ramos, J. Flix, M.C. Fouz, P. Garcia-Abia, O. Gonzalez Lopez, S. Goy Lopez, J.M. Hernandez, M.I. Josa, E. Navarro De Martino, A. Pérez-Calero Yzquierdo, J. Puerta Pelayo, A. Quintario Olmeda, I. Redondo, L. Romero, M.S. Soares

Universidad Autónoma de Madrid, Madrid, Spain
J.F. de Trocóniz, M. Missiroli, D. Moran

Universidad de Oviedo, Oviedo, Spain
J. Cuevas, J. Fernandez Menendez, I. Gonzalez Caballero, J.R. González Fernández, E. Palencia Cortezon, S. Sanchez Cruz, I. Suárez Andrés, J.M. Vizan Garcia

Instituto de Física de Cantabria (IFCA), CSIC-Universidad de Cantabria, Santander, Spain
I.J. Cabrillo, A. Calderon, J.R. Castiñeiras De Saa, E. Curras, M. Fernandez, J. Garcia-Ferrero, G. Gomez, A. Lopez Virto, J. Marco, C. Martinez Rivero, F. Matorras, J. Piedra Gomez, T. Rodrigo, A. Ruiz-Jimeno, L. Scodellaro, N. Trevisani, I. Vila, R. Vilar Cortabitarte

CERN, European Organization for Nuclear Research, Geneva, Switzerland
D. Abbaneo, E. Auffray, G. Auzinger, M. Bachtis, P. Baillon, A.H. Ball, D. Barney, P. Bloch, A. Bocci, A. Bonato, C. Botta, T. Camporesi, R. Castello, M. Cepeda, G. Cerminara, M. D'Alfonso, D. d'Enterria, A. Dabrowski, V. Daponte, A. David, M. De Gruttola, F. De Guio, A. De Roeck, E. Di Marco[44], M. Dobson, B. Dorney, T. du Pree, D. Duggan, M. Dünser, N. Dupont, A. Elliott-Peisert, S. Fartoukh, G. Franzoni, J. Fulcher, W. Funk, D. Gigi, K. Gill, M. Girone, F. Glege, D. Gulhan, S. Gundacker, M. Guthoff, J. Hammer, P. Harris, J. Hegeman, V. Innocente, P. Janot, H. Kirschenmann, V. Knünz, A. Kornmayer[14], M.J. Kortelainen, K. Kousouris, M. Krammer[1], P. Lecoq, C. Lourenço, M.T. Lucchini, L. Malgeri, M. Mannelli, A. Martelli, F. Meijers, S. Mersi, E. Meschi, F. Moortgat, S. Morovic, M. Mulders, H. Neugebauer, S. Orfanelli, L. Orsini, L. Pape, E. Perez, M. Peruzzi, A. Petrilli, G. Petrucciani, A. Pfeiffer, M. Pierini, A. Racz, T. Reis, G. Rolandi[45], M. Rovere, M. Ruan, H. Sakulin, J.B. Sauvan, C. Schäfer, C. Schwick, M. Seidel, A. Sharma, P. Silva, M. Simon, P. Sphicas[46], J. Steggemann, M. Stoye, Y. Takahashi, M. Tosi, D. Treille, A. Triossi, A. Tsirou, V. Veckalns[47], G.I. Veres[21], N. Wardle, A. Zagozdzinska[35], W.D. Zeuner

Paul Scherrer Institut, Villigen, Switzerland
W. Bertl, K. Deiters, W. Erdmann, R. Horisberger, Q. Ingram, H.C. Kaestli, D. Kotlinski, U. Langenegger, T. Rohe

Institute for Particle Physics, ETH Zurich, Zurich, Switzerland
F. Bachmair, L. Bäni, L. Bianchini, B. Casal, G. Dissertori, M. Dittmar, M. Donegà, P. Eller, C. Grab, C. Heidegger, D. Hits, J. Hoss, G. Kasieczka, P. Lecomte†, W. Lustermann, B. Mangano, M. Marionneau, P. Martinez Ruiz del Arbol, M. Masciovecchio, M.T. Meinhard, D. Meister, F. Micheli, P. Musella, F. Nessi-Tedaldi, F. Pandolfi, J. Pata, F. Pauss, G. Perrin, L. Perrozzi, M. Quittnat, M. Rossini, M. Schönenberger, A. Starodumov[48], V.R. Tavolaro, K. Theofilatos, R. Wallny

Universität Zürich, Zurich, Switzerland
T.K. Aarrestad, C. Amsler[49], L. Caminada, M.F. Canelli, A. De Cosa, C. Galloni, A. Hinzmann, T. Hreus, B. Kilminster, C. Lange, J. Ngadiuba, D. Pinna, G. Rauco, P. Robmann, D. Salerno, Y. Yang

National Central University, Chung-Li, Taiwan
V. Candelise, T.H. Doan, Sh. Jain, R. Khurana, M. Konyushikhin, C.M. Kuo, W. Lin, Y.J. Lu, A. Pozdnyakov, S.S. Yu

National Taiwan University (NTU), Taipei, Taiwan
Arun Kumar, P. Chang, Y.H. Chang, Y.W. Chang, Y. Chao, K.F. Chen, P.H. Chen, C. Dietz, F. Fiori, W.-S. Hou, Y. Hsiung, Y.F. Liu, R.-S. Lu, M. Miñano Moya, E. Paganis, A. Psallidas, J.f. Tsai, Y.M. Tzeng

Chulalongkorn University, Faculty of Science, Department of Physics, Bangkok, Thailand
B. Asavapibhop, G. Singh, N. Srimanobhas, N. Suwonjandee

Cukurova University, Adana, Turkey
A. Adiguzel, S. Cerci[50], S. Damarseckin, Z.S. Demiroglu, C. Dozen, I. Dumanoglu, S. Girgis, G. Gokbulut, Y. Guler, E. Gurpinar, I. Hos, E.E. Kangal[51], O. Kara, U. Kiminsu, M. Oglakci, G. Onengut[52], K. Ozdemir[53], D. Sunar Cerci[50], B. Tali[50], H. Topakli[54], S. Turkcapar, I.S. Zorbakir, C. Zorbilmez

Middle East Technical University, Physics Department, Ankara, Turkey
B. Bilin, S. Bilmis, B. Isildak[55], G. Karapinar[56], M. Yalvac, M. Zeyrek

Bogazici University, Istanbul, Turkey
E. Gülmez, M. Kaya[57], O. Kaya[58], E.A. Yetkin[59], T. Yetkin[60]

Istanbul Technical University, Istanbul, Turkey
A. Cakir, K. Cankocak, S. Sen[61]

Institute for Scintillation Materials of National Academy of Science of Ukraine, Kharkov, Ukraine
B. Grynyov

National Scientific Center, Kharkov Institute of Physics and Technology, Kharkov, Ukraine
L. Levchuk, P. Sorokin

University of Bristol, Bristol, United Kingdom
R. Aggleton, F. Ball, L. Beck, J.J. Brooke, D. Burns, E. Clement, D. Cussans, H. Flacher, J. Goldstein, M. Grimes, G.P. Heath, H.F. Heath, J. Jacob, L. Kreczko, C. Lucas, D.M. Newbold[62], S. Paramesvaran, A. Poll, T. Sakuma, S. Seif El Nasr-storey, D. Smith, V.J. Smith

Rutherford Appleton Laboratory, Didcot, United Kingdom
K.W. Bell, A. Belyaev[63], C. Brew, R.M. Brown, L. Calligaris, D. Cieri, D.J.A. Cockerill, J.A. Coughlan, K. Harder, S. Harper, E. Olaiya, D. Petyt, C.H. Shepherd-Themistocleous, A. Thea, I.R. Tomalin, T. Williams

Imperial College, London, United Kingdom
M. Baber, R. Bainbridge, O. Buchmuller, A. Bundock, D. Burton, S. Casasso, M. Citron, D. Colling, L. Corpe, P. Dauncey, G. Davies, A. De Wit, M. Della Negra, R. Di Maria, P. Dunne, A. Elwood, D. Futyan, Y. Haddad, G. Hall, G. Iles, T. James, R. Lane, C. Laner, R. Lucas[62], L. Lyons, A.-M. Magnan, S. Malik, L. Mastrolorenzo, J. Nash, A. Nikitenko[48], J. Pela, B. Penning,

M. Pesaresi, D.M. Raymond, A. Richards, A. Rose, C. Seez, S. Summers, A. Tapper, K. Uchida, M. Vazquez Acosta[64], T. Virdee[14], J. Wright, S.C. Zenz

Brunel University, Uxbridge, United Kingdom
J.E. Cole, P.R. Hobson, A. Khan, P. Kyberd, D. Leslie, I.D. Reid, P. Symonds, L. Teodorescu, M. Turner

Baylor University, Waco, USA
A. Borzou, K. Call, J. Dittmann, K. Hatakeyama, H. Liu, N. Pastika

The University of Alabama, Tuscaloosa, USA
O. Charaf, S.I. Cooper, C. Henderson, P. Rumerio

Boston University, Boston, USA
D. Arcaro, A. Avetisyan, T. Bose, D. Gastler, D. Rankin, C. Richardson, J. Rohlf, L. Sulak, D. Zou

Brown University, Providence, USA
G. Benelli, E. Berry, D. Cutts, A. Garabedian, J. Hakala, U. Heintz, J.M. Hogan, O. Jesus, E. Laird, G. Landsberg, Z. Mao, M. Narain, S. Piperov, S. Sagir, E. Spencer, R. Syarif

University of California, Davis, Davis, USA
R. Breedon, G. Breto, D. Burns, M. Calderon De La Barca Sanchez, S. Chauhan, M. Chertok, J. Conway, R. Conway, P.T. Cox, R. Erbacher, C. Flores, G. Funk, M. Gardner, W. Ko, R. Lander, C. Mclean, M. Mulhearn, D. Pellett, J. Pilot, F. Ricci-Tam, S. Shalhout, J. Smith, M. Squires, D. Stolp, M. Tripathi, S. Wilbur, R. Yohay

University of California, Los Angeles, USA
R. Cousins, P. Everaerts, A. Florent, J. Hauser, M. Ignatenko, D. Saltzberg, E. Takasugi, V. Valuev, M. Weber

University of California, Riverside, Riverside, USA
K. Burt, R. Clare, J. Ellison, J.W. Gary, G. Hanson, J. Heilman, P. Jandir, E. Kennedy, F. Lacroix, O.R. Long, M. Malberti, M. Olmedo Negrete, M.I. Paneva, A. Shrinivas, H. Wei, S. Wimpenny, B. R. Yates

University of California, San Diego, La Jolla, USA
J.G. Branson, G.B. Cerati, S. Cittolin, M. Derdzinski, R. Gerosa, A. Holzner, D. Klein, V. Krutelyov, J. Letts, I. Macneill, D. Olivito, S. Padhi, M. Pieri, M. Sani, V. Sharma, S. Simon, M. Tadel, A. Vartak, S. Wasserbaech[65], C. Welke, J. Wood, F. Würthwein, A. Yagil, G. Zevi Della Porta

University of California, Santa Barbara, Santa Barbara, USA
R. Bhandari, J. Bradmiller-Feld, C. Campagnari, A. Dishaw, V. Dutta, K. Flowers, M. Franco Sevilla, P. Geffert, C. George, F. Golf, L. Gouskos, J. Gran, R. Heller, J. Incandela, N. Mccoll, S.D. Mullin, A. Ovcharova, J. Richman, D. Stuart, I. Suarez, C. West, J. Yoo

California Institute of Technology, Pasadena, USA
D. Anderson, A. Apresyan, J. Bendavid, A. Bornheim, J. Bunn, Y. Chen, J. Duarte, J.M. Lawhorn, A. Mott, H.B. Newman, C. Pena, M. Spiropulu, J.R. Vlimant, S. Xie, R.Y. Zhu

Carnegie Mellon University, Pittsburgh, USA
M.B. Andrews, V. Azzolini, B. Carlson, T. Ferguson, M. Paulini, J. Russ, M. Sun, H. Vogel, I. Vorobiev

University of Colorado Boulder, Boulder, USA
J.P. Cumalat, W.T. Ford, F. Jensen, A. Johnson, M. Krohn, T. Mulholland, K. Stenson, S.R. Wagner

Cornell University, Ithaca, USA
J. Alexander, J. Chaves, J. Chu, S. Dittmer, K. Mcdermott, N. Mirman, G. Nicolas Kaufman, J.R. Patterson, A. Rinkevicius, A. Ryd, L. Skinnari, L. Soffi, S.M. Tan, Z. Tao, J. Thom, J. Tucker, P. Wittich, M. Zientek

Fairfield University, Fairfield, USA
D. Winn

Fermi National Accelerator Laboratory, Batavia, USA
S. Abdullin, M. Albrow, G. Apollinari, S. Banerjee, L.A.T. Bauerdick, A. Beretvas, J. Berryhill, P.C. Bhat, G. Bolla, K. Burkett, J.N. Butler, H.W.K. Cheung, F. Chlebana, S. Cihangir, M. Cremonesi, V.D. Elvira, I. Fisk, J. Freeman, E. Gottschalk, L. Gray, D. Green, S. Grünendahl, O. Gutsche, D. Hare, R.M. Harris, S. Hasegawa, J. Hirschauer, Z. Hu, B. Jayatilaka, S. Jindariani, M. Johnson, U. Joshi, B. Klima, B. Kreis, S. Lammel, J. Linacre, D. Lincoln, R. Lipton, T. Liu, R. Lopes De Sá, J. Lykken, K. Maeshima, N. Magini, J.M. Marraffino, S. Maruyama, D. Mason, P. McBride, P. Merkel, S. Mrenna, S. Nahn, C. Newman-Holmes†, V. O'Dell, K. Pedro, O. Prokofyev, G. Rakness, L. Ristori, E. Sexton-Kennedy, A. Soha, W.J. Spalding, L. Spiegel, S. Stoynev, N. Strobbe, L. Taylor, S. Tkaczyk, N.V. Tran, L. Uplegger, E.W. Vaandering, C. Vernieri, M. Verzocchi, R. Vidal, M. Wang, H.A. Weber, A. Whitbeck

University of Florida, Gainesville, USA
D. Acosta, P. Avery, P. Bortignon, D. Bourilkov, A. Brinkerhoff, A. Carnes, M. Carver, D. Curry, S. Das, R.D. Field, I.K. Furic, J. Konigsberg, A. Korytov, P. Ma, K. Matchev, H. Mei, P. Milenovic[66], G. Mitselmakher, D. Rank, L. Shchutska, D. Sperka, L. Thomas, J. Wang, S. Wang, J. Yelton

Florida International University, Miami, USA
S. Linn, P. Markowitz, G. Martinez, J.L. Rodriguez

Florida State University, Tallahassee, USA
A. Ackert, J.R. Adams, T. Adams, A. Askew, S. Bein, B. Diamond, S. Hagopian, V. Hagopian, K.F. Johnson, A. Khatiwada, H. Prosper, A. Santra, M. Weinberg

Florida Institute of Technology, Melbourne, USA
M.M. Baarmand, V. Bhopatkar, S. Colafranceschi[67], M. Hohlmann, D. Noonan, T. Roy, F. Yumiceva

University of Illinois at Chicago (UIC), Chicago, USA
M.R. Adams, L. Apanasevich, D. Berry, R.R. Betts, I. Bucinskaite, R. Cavanaugh, O. Evdokimov, L. Gauthier, C.E. Gerber, D.J. Hofman, P. Kurt, C. O'Brien, I.D. Sandoval Gonzalez, P. Turner, N. Varelas, H. Wang, Z. Wu, M. Zakaria, J. Zhang

The University of Iowa, Iowa City, USA
B. Bilki[68], W. Clarida, K. Dilsiz, S. Durgut, R.P. Gandrajula, M. Haytmyradov, V. Khristenko, J.-P. Merlo, H. Mermerkaya[69], A. Mestvirishvili, A. Moeller, J. Nachtman, H. Ogul, Y. Onel, F. Ozok[70], A. Penzo, C. Snyder, E. Tiras, J. Wetzel, K. Yi

Johns Hopkins University, Baltimore, USA
I. Anderson, B. Blumenfeld, A. Cocoros, N. Eminizer, D. Fehling, L. Feng, A.V. Gritsan, P. Maksimovic, M. Osherson, J. Roskes, U. Sarica, M. Swartz, M. Xiao, Y. Xin, C. You

The University of Kansas, Lawrence, USA
A. Al-bataineh, P. Baringer, A. Bean, J. Bowen, C. Bruner, J. Castle, R.P. Kenny III, A. Kropivnitskaya, D. Majumder, W. Mcbrayer, M. Murray, S. Sanders, R. Stringer, J.D. Tapia Takaki, Q. Wang

Kansas State University, Manhattan, USA
A. Ivanov, K. Kaadze, S. Khalil, M. Makouski, Y. Maravin, A. Mohammadi, L.K. Saini, N. Skhirtladze, S. Toda

Lawrence Livermore National Laboratory, Livermore, USA
D. Lange, F. Rebassoo, D. Wright

University of Maryland, College Park, USA
C. Anelli, A. Baden, O. Baron, A. Belloni, B. Calvert, S.C. Eno, C. Ferraioli, J.A. Gomez, N.J. Hadley, S. Jabeen, R.G. Kellogg, T. Kolberg, J. Kunkle, Y. Lu, A.C. Mignerey, Y.H. Shin, A. Skuja, M.B. Tonjes, S.C. Tonwar

Massachusetts Institute of Technology, Cambridge, USA
D. Abercrombie, B. Allen, A. Apyan, R. Barbieri, A. Baty, R. Bi, K. Bierwagen, S. Brandt, W. Busza, I.A. Cali, Z. Demiragli, L. Di Matteo, G. Gomez Ceballos, M. Goncharov, D. Hsu, Y. Iiyama, G.M. Innocenti, M. Klute, D. Kovalskyi, K. Krajczar, Y.S. Lai, Y.-J. Lee, A. Levin, P.D. Luckey, A.C. Marini, C. Mcginn, C. Mironov, S. Narayanan, X. Niu, C. Paus, C. Roland, G. Roland, J. Salfeld-Nebgen, G.S.F. Stephans, K. Sumorok, K. Tatar, M. Varma, D. Velicanu, J. Veverka, J. Wang, T.W. Wang, B. Wyslouch, M. Yang, V. Zhukova

University of Minnesota, Minneapolis, USA
A.C. Benvenuti, R.M. Chatterjee, A. Evans, A. Finkel, A. Gude, P. Hansen, S. Kalafut, S.C. Kao, Y. Kubota, Z. Lesko, J. Mans, S. Nourbakhsh, N. Ruckstuhl, R. Rusack, N. Tambe, J. Turkewitz

University of Mississippi, Oxford, USA
J.G. Acosta, S. Oliveros

University of Nebraska-Lincoln, Lincoln, USA
E. Avdeeva, R. Bartek, K. Bloom, S. Bose, D.R. Claes, A. Dominguez, C. Fangmeier, R. Gonzalez Suarez, R. Kamalieddin, D. Knowlton, I. Kravchenko, A. Malta Rodrigues, F. Meier, J. Monroy, J.E. Siado, G.R. Snow, B. Stieger

State University of New York at Buffalo, Buffalo, USA
M. Alyari, J. Dolen, J. George, A. Godshalk, C. Harrington, I. Iashvili, J. Kaisen, A. Kharchilava, A. Kumar, A. Parker, S. Rappoccio, B. Roozbahani

Northeastern University, Boston, USA
G. Alverson, E. Barberis, D. Baumgartel, A. Hortiangtham, A. Massironi, D.M. Morse, D. Nash, T. Orimoto, R. Teixeira De Lima, D. Trocino, R.-J. Wang, D. Wood

Northwestern University, Evanston, USA
S. Bhattacharya, K.A. Hahn, A. Kubik, A. Kumar, J.F. Low, N. Mucia, N. Odell, B. Pollack, M.H. Schmitt, K. Sung, M. Trovato, M. Velasco

University of Notre Dame, Notre Dame, USA
N. Dev, M. Hildreth, K. Hurtado Anampa, C. Jessop, D.J. Karmgard, N. Kellams, K. Lannon, N. Marinelli, F. Meng, C. Mueller, Y. Musienko[36], M. Planer, A. Reinsvold, R. Ruchti, G. Smith, S. Taroni, N. Valls, M. Wayne, M. Wolf, A. Woodard

The Ohio State University, Columbus, USA
J. Alimena, L. Antonelli, J. Brinson, B. Bylsma, L.S. Durkin, S. Flowers, B. Francis, A. Hart, C. Hill, R. Hughes, W. Ji, B. Liu, W. Luo, D. Puigh, B.L. Winer, H.W. Wulsin

Princeton University, Princeton, USA
S. Cooperstein, O. Driga, P. Elmer, J. Hardenbrook, P. Hebda, J. Luo, D. Marlow, T. Medvedeva, K. Mei, M. Mooney, J. Olsen, C. Palmer, P. Piroué, D. Stickland, C. Tully, A. Zuranski

University of Puerto Rico, Mayaguez, USA
S. Malik

Purdue University, West Lafayette, USA
A. Barker, V.E. Barnes, S. Folgueras, L. Gutay, M.K. Jha, M. Jones, A.W. Jung, K. Jung, D.H. Miller, N. Neumeister, B.C. Radburn-Smith, X. Shi, J. Sun, A. Svyatkovskiy, F. Wang, W. Xie, L. Xu

Purdue University Calumet, Hammond, USA
N. Parashar, J. Stupak

Rice University, Houston, USA
A. Adair, B. Akgun, Z. Chen, K.M. Ecklund, F.J.M. Geurts, M. Guilbaud, W. Li, B. Michlin, M. Northup, B.P. Padley, R. Redjimi, J. Roberts, J. Rorie, Z. Tu, J. Zabel

University of Rochester, Rochester, USA
B. Betchart, A. Bodek, P. de Barbaro, R. Demina, Y.t. Duh, T. Ferbel, M. Galanti, A. Garcia-Bellido, J. Han, O. Hindrichs, A. Khukhunaishvili, K.H. Lo, P. Tan, M. Verzetti

Rutgers, The State University of New Jersey, Piscataway, USA
J.P. Chou, E. Contreras-Campana, Y. Gershtein, T.A. Gómez Espinosa, E. Halkiadakis, M. Heindl, D. Hidas, E. Hughes, S. Kaplan, R. Kunnawalkam Elayavalli, S. Kyriacou, A. Lath, K. Nash, H. Saka, S. Salur, S. Schnetzer, D. Sheffield, S. Somalwar, R. Stone, S. Thomas, P. Thomassen, M. Walker

University of Tennessee, Knoxville, USA
M. Foerster, J. Heideman, G. Riley, K. Rose, S. Spanier, K. Thapa

Texas A&M University, College Station, USA
O. Bouhali[71], A. Celik, M. Dalchenko, M. De Mattia, A. Delgado, S. Dildick, R. Eusebi, J. Gilmore, T. Huang, E. Juska, T. Kamon[72], R. Mueller, Y. Pakhotin, R. Patel, A. Perloff, L. Perniè, D. Rathjens, A. Rose, A. Safonov, A. Tatarinov, K.A. Ulmer

Texas Tech University, Lubbock, USA
N. Akchurin, C. Cowden, J. Damgov, C. Dragoiu, P.R. Dudero, J. Faulkner, S. Kunori, K. Lamichhane, S.W. Lee, T. Libeiro, S. Undleeb, I. Volobouev, Z. Wang

Vanderbilt University, Nashville, USA
A.G. Delannoy, S. Greene, A. Gurrola, R. Janjam, W. Johns, C. Maguire, A. Melo, H. Ni, P. Sheldon, S. Tuo, J. Velkovska, Q. Xu

University of Virginia, Charlottesville, USA
M.W. Arenton, P. Barria, B. Cox, J. Goodell, R. Hirosky, A. Ledovskoy, H. Li, C. Neu, T. Sinthuprasith, X. Sun, Y. Wang, E. Wolfe, F. Xia

Wayne State University, Detroit, USA
C. Clarke, R. Harr, P.E. Karchin, P. Lamichhane, J. Sturdy

University of Wisconsin - Madison, Madison, WI, USA
D.A. Belknap, S. Dasu, L. Dodd, S. Duric, B. Gomber, M. Grothe, M. Herndon, A. Hervé, P. Klabbers, A. Lanaro, A. Levine, K. Long, R. Loveless, I. Ojalvo, T. Perry, G.A. Pierro, G. Polese, T. Ruggles, A. Savin, A. Sharma, N. Smith, W.H. Smith, D. Taylor, N. Woods

†: Deceased
1: Also at Vienna University of Technology, Vienna, Austria
2: Also at State Key Laboratory of Nuclear Physics and Technology, Peking University, Beijing, China
3: Also at Institut Pluridisciplinaire Hubert Curien, Université de Strasbourg, Université de Haute Alsace Mulhouse, CNRS/IN2P3, Strasbourg, France
4: Also at Universidade Estadual de Campinas, Campinas, Brazil
5: Also at Université Libre de Bruxelles, Bruxelles, Belgium
6: Also at Deutsches Elektronen-Synchrotron, Hamburg, Germany
7: Also at Joint Institute for Nuclear Research, Dubna, Russia
8: Also at Helwan University, Cairo, Egypt
9: Now at Zewail City of Science and Technology, Zewail, Egypt
10: Now at Fayoum University, El-Fayoum, Egypt
11: Also at British University in Egypt, Cairo, Egypt
12: Now at Ain Shams University, Cairo, Egypt
13: Also at Université de Haute Alsace, Mulhouse, France
14: Also at CERN, European Organization for Nuclear Research, Geneva, Switzerland
15: Also at Skobeltsyn Institute of Nuclear Physics, Lomonosov Moscow State University, Moscow, Russia
16: Also at Tbilisi State University, Tbilisi, Georgia
17: Also at RWTH Aachen University, III. Physikalisches Institut A, Aachen, Germany
18: Also at University of Hamburg, Hamburg, Germany
19: Also at Brandenburg University of Technology, Cottbus, Germany
20: Also at Institute of Nuclear Research ATOMKI, Debrecen, Hungary
21: Also at MTA-ELTE Lendület CMS Particle and Nuclear Physics Group, Eötvös Loránd University, Budapest, Hungary
22: Also at University of Debrecen, Debrecen, Hungary
23: Also at Indian Institute of Science Education and Research, Bhopal, India
24: Also at Institute of Physics, Bhubaneswar, India
25: Also at University of Visva-Bharati, Santiniketan, India
26: Also at University of Ruhuna, Matara, Sri Lanka
27: Also at Isfahan University of Technology, Isfahan, Iran
28: Also at University of Tehran, Department of Engineering Science, Tehran, Iran
29: Also at Plasma Physics Research Center, Science and Research Branch, Islamic Azad University, Tehran, Iran
30: Also at Università degli Studi di Siena, Siena, Italy
31: Also at Purdue University, West Lafayette, USA
32: Also at International Islamic University of Malaysia, Kuala Lumpur, Malaysia
33: Also at Malaysian Nuclear Agency, MOSTI, Kajang, Malaysia
34: Also at Consejo Nacional de Ciencia y Tecnología, Mexico city, Mexico
35: Also at Warsaw University of Technology, Institute of Electronic Systems, Warsaw, Poland
36: Also at Institute for Nuclear Research, Moscow, Russia
37: Now at National Research Nuclear University 'Moscow Engineering Physics Institute' (MEPhI), Moscow, Russia
38: Also at St. Petersburg State Polytechnical University, St. Petersburg, Russia

39: Also at University of Florida, Gainesville, USA
40: Also at P.N. Lebedev Physical Institute, Moscow, Russia
41: Also at California Institute of Technology, Pasadena, USA
42: Also at Budker Institute of Nuclear Physics, Novosibirsk, Russia
43: Also at Faculty of Physics, University of Belgrade, Belgrade, Serbia
44: Also at INFN Sezione di Roma; Università di Roma, Roma, Italy
45: Also at Scuola Normale e Sezione dell'INFN, Pisa, Italy
46: Also at National and Kapodistrian University of Athens, Athens, Greece
47: Also at Riga Technical University, Riga, Latvia
48: Also at Institute for Theoretical and Experimental Physics, Moscow, Russia
49: Also at Albert Einstein Center for Fundamental Physics, Bern, Switzerland
50: Also at Adiyaman University, Adiyaman, Turkey
51: Also at Mersin University, Mersin, Turkey
52: Also at Cag University, Mersin, Turkey
53: Also at Piri Reis University, Istanbul, Turkey
54: Also at Gaziosmanpasa University, Tokat, Turkey
55: Also at Ozyegin University, Istanbul, Turkey
56: Also at Izmir Institute of Technology, Izmir, Turkey
57: Also at Marmara University, Istanbul, Turkey
58: Also at Kafkas University, Kars, Turkey
59: Also at Istanbul Bilgi University, Istanbul, Turkey
60: Also at Yildiz Technical University, Istanbul, Turkey
61: Also at Hacettepe University, Ankara, Turkey
62: Also at Rutherford Appleton Laboratory, Didcot, United Kingdom
63: Also at School of Physics and Astronomy, University of Southampton, Southampton, United Kingdom
64: Also at Instituto de Astrofísica de Canarias, La Laguna, Spain
65: Also at Utah Valley University, Orem, USA
66: Also at University of Belgrade, Faculty of Physics and Vinca Institute of Nuclear Sciences, Belgrade, Serbia
67: Also at Facoltà Ingegneria, Università di Roma, Roma, Italy
68: Also at Argonne National Laboratory, Argonne, USA
69: Also at Erzincan University, Erzincan, Turkey
70: Also at Mimar Sinan University, Istanbul, Istanbul, Turkey
71: Also at Texas A&M University at Qatar, Doha, Qatar
72: Also at Kyungpook National University, Daegu, Korea